EXAMENSARBETE I GEOLOGI VID LUNDS UNIVERSITET

Berggrundsgeologi

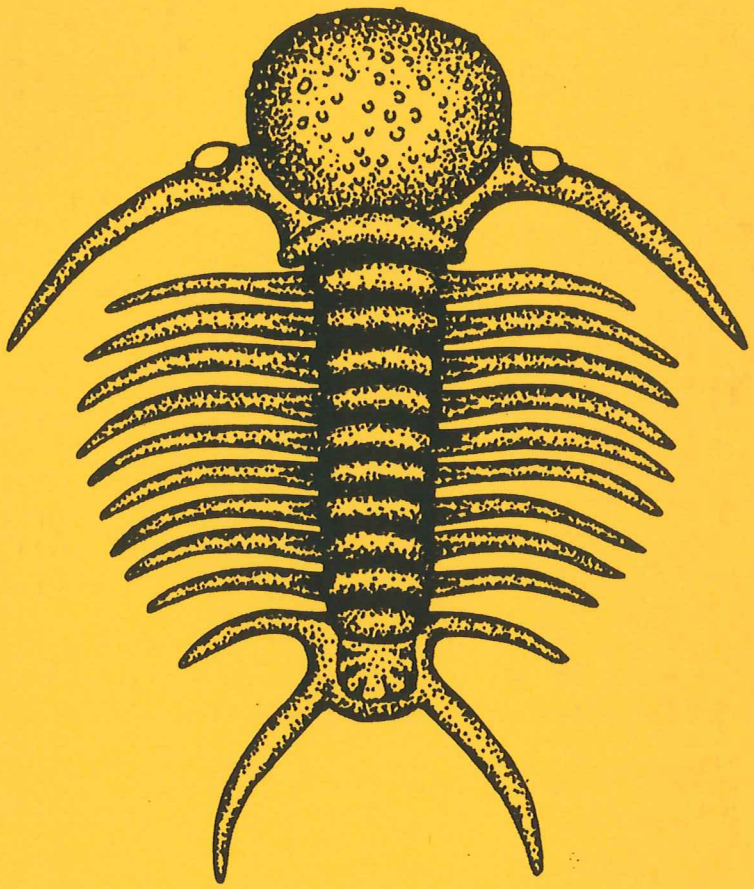

Correlation between diagenesis and sedimentary facies of the Bentheim Sandstone, the Schoonebeek field, The Netherlands

Pär Malmborg

Examensarbete, 20 p Nr 150
Institutionen, Lunds Universitet

CODEN: SE-LUNBDS/NBGO-02/5150+30S

EXAMENSARBETE I GEOLOGI VID LUNDS UNIVERSITET

Berggrundsgeologi

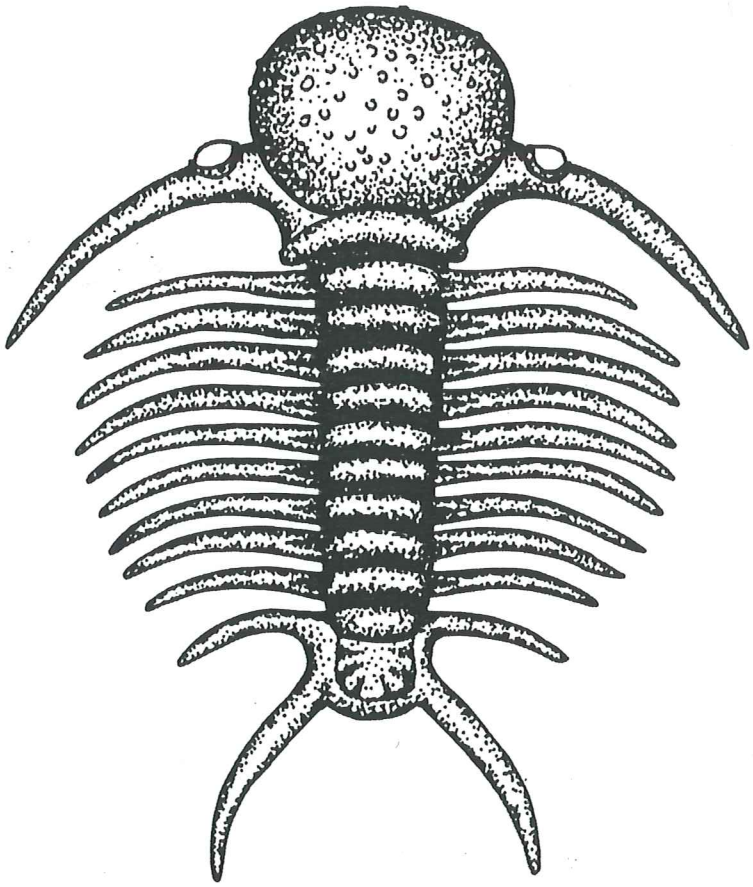

Correlation between diagenesis and sedimentary facies of the Bentheim Sandstone, the Schoonebeek field, The Netherlands

Pär Malmborg

Lund 2002 **Examensarbete, 20 p** **Nr 150**
Geologiska Institutionen, Lunds Universitet

Correlation between diagenesis and sedimentary facies of the Bentheim Sandstone, the Schoonebeek field, The Netherlands

Petrographic and sedimentological re-evaluation of a petroleum reservoir

PÄR MALMBORG

Malmborg, P., 2002: Correlation between diagenesis and sedimentary facies of the Bentheim Sandstone, the Schoonebeek field, The Netherlands. *Examensarbete i geologi vid Lunds Universitet, avd för Berggrundsgeologi Nr 150, 30 pp.*

Abstract: The Valanginian (Lower Cretaceous) Bentheim succession of the Schoonebeek field is deposited in a shallow-marine environment along the southern and southwestern coast of the Lower Saxony Basin in eastern Netherlands. Three cores from Schoonebeek field, selected by NAM (Nederlandse Aardolie Maatschappij), and a number of samples from an outcrop in the Bentheim Sandstone at Gildehaus were studied. Interpretations of the depositional environments were made based on the three cores. Bioturbated, massive, heterolithic and open marine clastic sediments were distinguished. These categories correspond to those of the new stratigraphical division of the Emsland area. The porosity and permeability of the Bentheim sandstone is largely linked to depositional facies. Diagenesis has affected the petrophysical properties mainly through carbonate cementation and leaching of detrital grains. The effect of mechanical compaction was minor because of the stable (quartz rich) detrital composition of the sand. The early precipitation of calcite cement in a number of thin layers caused the development of impermeable layers.

During the maturation of the Berriasian source rocks aggressive pore fluids were expelled, which enhanced the porosity of the Bentheim Sandstone. Later the charging of hydrocarbon into the Bentheim Sandstone initiated the process of blocking "pure" nucleus, which inhibited quartz cementation and authigenic clay precipitation in the sandstones of the Schoonebeek field. The leaching processes, the development of secondary porosity, and the low content of authigenic clay suggest that fluid transport removed ions in a semi-closed or open diagenetic system. The depositional and diagenetic properties have resulted in good reservoir quality of the Bentheim Sandstone, especially within the massive sandstone. The carbonate-cemented layers represent stratabound impermeable layers, which probably were developed by local diffusional redistribution of biogenic carbonate. The abundance of corroded detrital grains and calcite cement in the Bentheim Sandstone suggest that at least the carbonate-cemented layers were more extensive prior to the maturation of hydrocarbon.

Keywords: Bentheim Sandstone, sedimentary facies, diagenesis, petroleum reservoir, Lower Cretaceous, Valanginian, Lower Saxony Basin, Schoonebeek, Gildehaus.

P. Malmborg, Department of Geology, Division of Geology, Lund University, Sölvegatan 13, SE-223 62 Lund, Sweden. E-mail: parmalmborg@hotmail.com.

The Valangianan (Lower Cretaceous) Bentheim Sandstone was deposited in a shallow-marine environment along the southern and southwestern coast of the Lower Saxony Basin. The Schoonebeek field, which includes the Bentheim Sandstone reservoir units was yielded high-viscosity oil and is one of the largest oilfields onshore Northwestern Europe. During petroleum production, heterogeneity of the reservoir sandstone has caused water break-through and diminished the production.

In detail, most sandstone reservoirs are more heterogeneous with respect to their petrophysical properties than previously expected. The heterogeneity is a result of depositional variability and subsequent differential diagenesis. Evidently, the Schoonebeek reservoir body consists of strata with different permeability (i.e., different flow units). Carbonate-cemented layers or horizons with carbonate concretions may form important fluid barriers. A better reservoir model has to be developed for the Bentheim Sandstone, taking into account the permeability heterogeneity. Improved technology, horizontal drilling techniques together with improved geological and fluid flow models are newly develop methods for secondary recovery and indeed needed to bring the reservoir back in production.

Aims of the research project

The aims of the study are:

- To investigate the petrophysical properties and the heterogeneity of the reservoir properties of the three cores from the Bentheim Sandstone in the Schoonebeek field, eastern Netherlands.
- To establish a paragenetic sequence of diagenetic features and to construct a basic diagenetic model.
- To quantify the effects of the diagenetic processes on the main petrophysical properties (porosity and permeability).
- To verify the influence of the depositional facies (textures, composition and structures) on the diagenetic processes (and thus on petrophysical properties), and to construct a model that correlates diagenesis and petrophysical properties to facies.
- The quantification of detrital and authigenic components (using standard microscopy, CL and SEM microscopy and image analyses next to traditional point counting).
- To couple the results to chemical modelling (in order to derive mass-balanced models for diagenesis)
- To unravel the causal relationship between the observed diagenetic features and chemical-physical processes involved.

Lower Saxony Basin

Geological history

The Lower Saxony Basin (LSB) is roughly 400 km long and 100 km wide and constitutes a group of NW-SE oriented basins and troughs, situated to the north of the Rhenish Massif (Mutterlose & Bornemann 2000). The basin margins are formed by the Pompeck swell to the north, the East Netherlands High to the west and the East Brandenburg High to the east (Fig. 1).

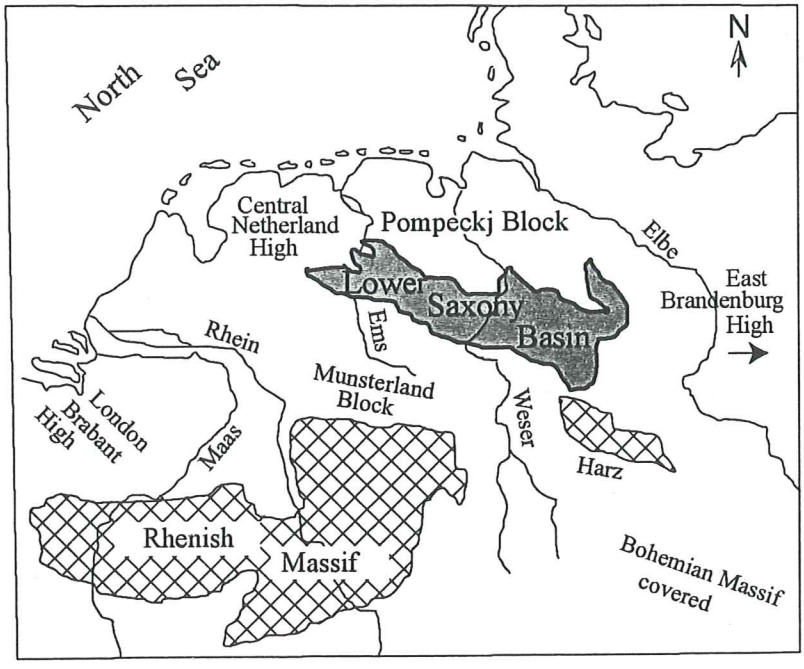

Fig. 1. Location of Lower Saxony Basin in northwestern Germany and eastern Netherlands (after Kockel et al. 1994).

Fig 2. Map of the area with locations of Schoonebeek (subcrop) and Gildehaus (outcrop).

The development of the Lower Saxony Basin (LSB) is related to crustal extension in the North Sea area during late Middle to early Late Jurassic times. This was followed by subsidence and later inversion, which affected the basin until the Cenozoic (Parnell et al. 1996). The subsidence started in Late Jurassic times (early Kimmeridgian) and continued throughout to the late Aptian times (Early Cretaceous), after which there was a decrease in tectonic activity until the late Turonian. In early Coniacian an inversion of the basin began, which locally in LSB already took place in the early Turonian. The inversion peaked in the Santonian and continued into Campanian times. Continued inversion affected the basin in the latest Cretaceous and Early Tertiary, which converted the former "graben" into the present LSB (Mutterlose & Bornemann 2000). Mutterlose & Bornemann (2000) estimated that about 2000 m of Lower Cretaceous sediments accumulated in this epeirogenic basin. Based on the variation in thickness and lithology, they have divided the basin into five sub-basins. The western part of the LSB including the Emsland area (i.e., the Bentheim-Meppen-Groningen) constitutes one of these five sub-basins, where the Schoonebeek field and the three cores are located (Schoonebeek 495, 586 and 590) (Fig. 2).

Regional setting of the Emsland area

Early Cretaceous sediment

In the area of the German-Dutch borderland, sediments from the earliest Cretaceous age (Berriasian- Barremian) are widespread. This study is focussed on the Bentheim Sandstone of Valanginian age, which is the principal reservoir sandstone body in the Schoonebeek field (Fig. 3). Sediments from the Early Cretaceous (Aptian-Albian) are uncommon in the area. All outcrops that are situated in the Emsland can be related to the east- west striking salt anticlines (Wonham et al. 1997).

Berriasian eustarine sediments with marine influence

Berriasian estuarine sediments cover large areas in the Emsland, compared to contemporary sediments in other parts of the LSB. The early Berrasian represents a period with a relative sea level low stand, which is reflected by a change in the depositional environment from restricted and evaporitic marine conditions to brackish and fresh water conditions in the Wealden area (Betz et al. 1986). Despite the lowering of the base level, sedimentation continued in the actively subsiding parts of the LSB. Between early and late Berriasian time, several short periods of marine flooding started, which continued throughout the late Berriasian. There are many opinions on the provenance of these marine strata (Wonham et al. 1997; Mutterlose & Bornemann 2000) but all assume that they come from the west via the East Netherlands High. These presumptions are based on the fact that the marine sediments pinch out towards the middle and eastern parts of the basin (Strauss et al. 1993).

Valanginian marine and deltaic sediment

According to Hinze (1988) all Valanginian deposits are concentrated along salt anticlines and the prevailing opinion is that the start of the Valanginain represents a transgression, from the North Sea area that protruded via the East Netherlands High to the Emsland area. In earliest Valanginian fully marine depositional conditions were established, which later were interrupted by regression, and followed by another extensive transgression in the lowermost upper Valanginian. During the Valanginian transgression a thick succession of marine claystones was deposited in the LSB, including a number of intercalated sandstones such as the Bentheim Sandstone, the *Dichotomites* Sandstone and the Grenz Sandstone. These are believed to be of deltaic and shoreline origin, deposited along the basin margins (Betz et al. 1986).

The Bentheim Sandstone

The early Valanginian Bentheim Sandstone is a shallow-marine sandstone deposited in a high-energy, near-shore environment (Mutterlose & Bornemann 2000). All provenance studies are focussed on detrital clastics and Füchtbauer (1955 1963) assumed a southern location of the sediment source area, whereas Kemper (1976 1992) believed in multiple sediment sources areas for the sandstones in the Bentheim area.

In the Romberg Quarry at Gildehaus, the Bentheim Sandstone has been divided into three main lithostratigraphic units (Kemper 1968 1976; Kortmann 1983). These units are the Lower Bentheim Sandstone, the Romberg clay and the Upper Bentheim Sandstone. Wonham et al. (1997) has further subdivided the Lower Bentheim Sandstone into four members, i.e. the Lower bioturbated zone, the Basisbank, the Heterolithic facies and the Haupt sandstone.

The two massive sandstones of the Lower Bentheim Sandstone, the Basisbank and the Haupt sandstone are assumed to be turbiditic (Basisbank) and of beach barri-

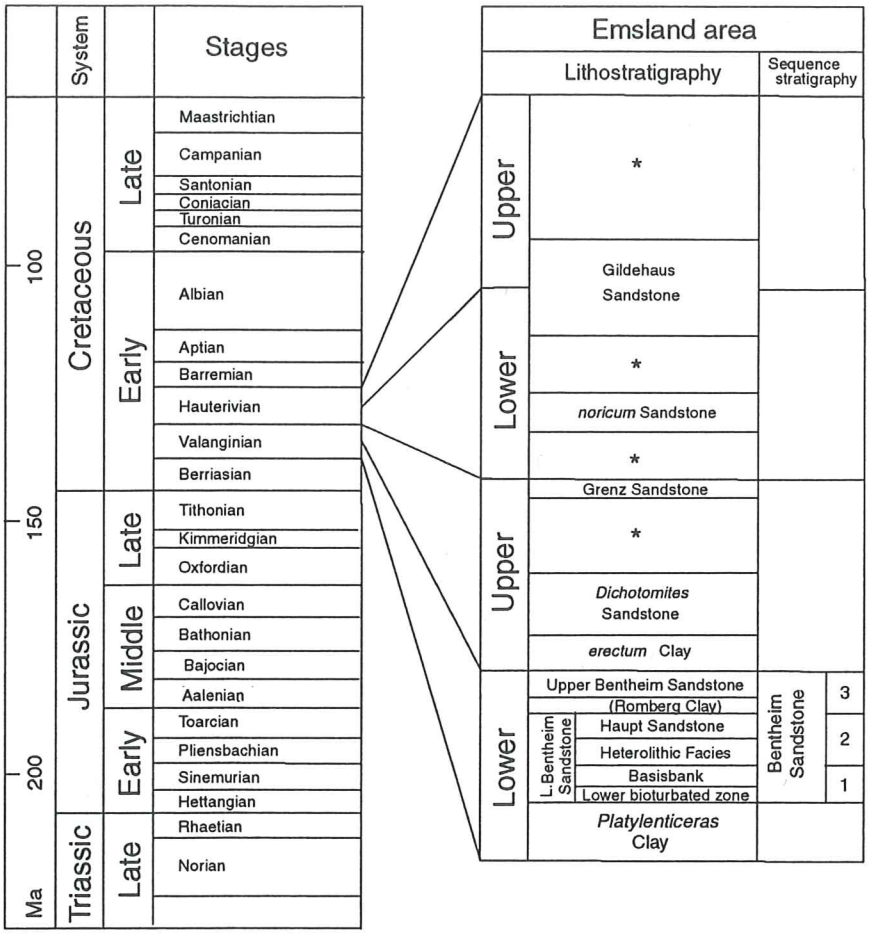

Fig. 3. The stages of the Emsland area with lithostratigraphic and sequence stratigraphic division (after Mutterlose & Bornemann 2000).

er sand origin (Haupt sandstone), respectively. Coast parallel currents (Mutterlose & Bornemann 2000) deposited the Haupt sandstone. Recently several articles have treated the Bentheim sandstone in a sequence stratigraphic framework (Mutterlose et al. 1995, Wonham et al. 1997 and Stadler 1998) and a new depositional model has been proposed by Mutterlose & Bornemann (2000). Accordingly, the Bentheim Sandstone has been divided into three sequences (Bentheim 1-3), which represent three regressive-transgressive cycles and all three are bounded by biostratigraphically defined maximum flooding surfaces. Tidal influence has been suspected in all three sequences. The sequences Bentheim 1 and Bentheim 2 (Lower Bentheim Sandstone) are deposited under high-energy conditions and correspond to the Basisbank and the Haupt Sandstone of the lithostratigraphical subdivision, whereas the Bentheim 3 sequence is deposited in the lower tidal zone, characterised by lower energy conditions. This unit corresponds to the Upper Bentheim Sandstone of the old subdivision (Mutterlose & Bornemann 2000). The depositional pattern of the Bentheim 1 was controlled and influenced by tectonic forces. The subsidence rate varies in the basin during this period and it is believed that a more heterolithic facies was developed on structural highs in low-energy environments, whereas in the central parts, which were affected by rapid subsidence, coarser grained sand in large-scale cross-stratified sandstone was developed.

The Dichotomites and Grenz Sandstone

In the upper Valanginian, the *Dichotomites* Sandstone and Grenz Sandstone show higher concentrations of clay. Mutterlose & Bornemann (2000) interpreted these deposits as retrograding facies and related this pattern to the overall picture of the increasing subsidence rate of the basin during the Valanginian.

Hauterivian marine sediment deposited during transgressive cycles

The general idea of sediments of this age (Wonham et al. 1997 and Mutterlose & Bornemann 2000) is that the deposition occurred along the margins of the salt anticlines. The Hauterivian succession consists of three transgressive stages. Two sandstones developed in this unit in the Emsland area, i.e., the *noricum* Sandstone and the Gildehaus Sandstone of mid early Hauterivian age.

Berremian clay sediment deposited in a regressive phase

The sediment deposited during this the Barremian is related to regressive conditions and occurs in the Brechte syncline between Ochtrup, Gronau and Bentheim. Most of the deposits are organic rich clays, with a thickness of 400 m (Mutterlose & Bornemann 2000).

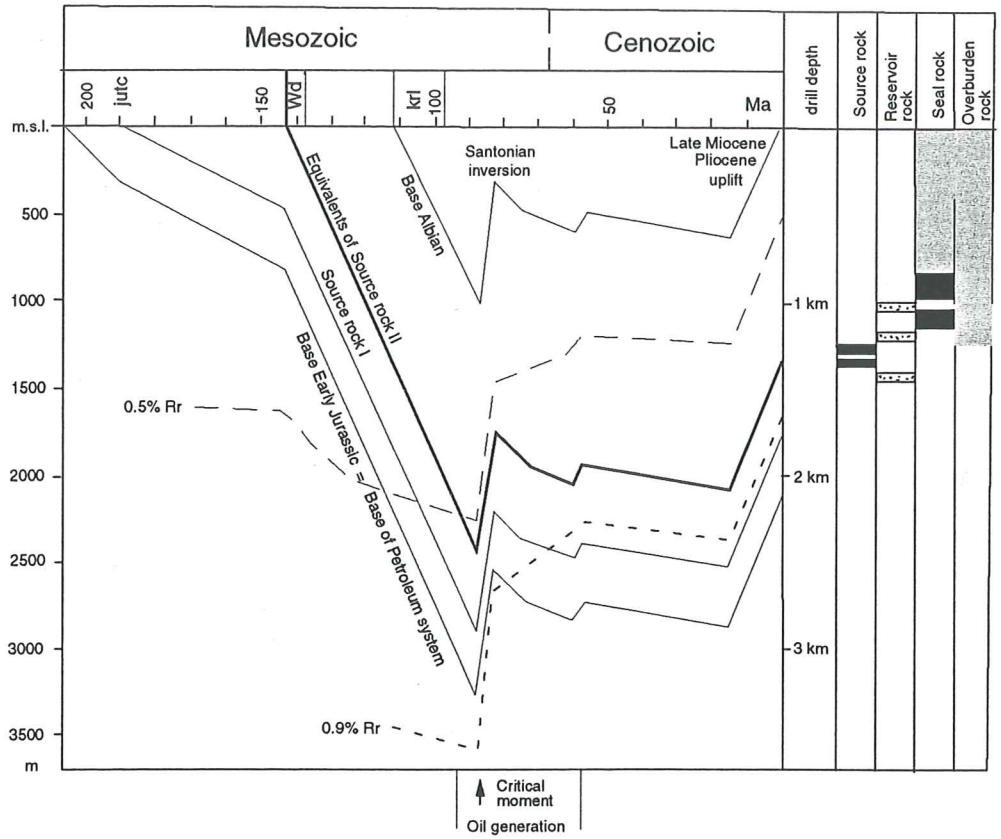

Fig. 4. The burial history of the source rock I and II, of which the latter experienced the oil window from 92 to 56 Ma (after Kockel et al. 1994).

Burial history

Parnell et al. (1996) reconstructed the burial history of the LSB and modelled that the peak of hydrocarbon generation in the Berriasian deposit occurred before its maximum burial depth was reached. The burial history indicated that the Berriasian papershales (source rock II) passed the oil generative window between 92 and 56 Ma (Fig. 4) (Kockel et al. 1994).

Source rocks

The lacustrine Berriasian succession acts as the source rock for the oil in the Bentheim Sandstone. The deposition was related to several short-lived periods of marine flooding, where the source rock was restricted to its western parts of the LSB (west of the river Weser) and to the western margin, where it oversteps the Posidonia Shale (source rock I) distribution area to the west of the Ems River (Kockel et al. 1994). The geographical setting of Schoonebeck field implies that the lacustrine Berriasian succession encompasses the only source rocks in the Schoonebeek field, whereas in the area between the Ems and Weser River a mixture of Berriasian and Posidonia origin oil types can be found. In the latter area the two thermally mature source rock units (I+II) are present. There, the reservoir rocks (Valanginian sandstones) are found just above the lacustrine Berriasian succession (Kockel et al. 1994).

According to Kockel et al. (1994) the mean TOC (Total Organic Content) value is 7 wt. % in the western area. The kerogen is type I, but type II is increasingly abundant as the Weser River is approached. Further to the east of the LSB kerogen type III predominates. The organic matter of the lacustrine Berriasian papershales is characterised by a value of -32‰, with a thermal maturity ranging from immature (<0.5% R_0) along the northern margin of the basin to postmature (<0.9% R_0) in the basin centre (Kockel et al. 1994). The mean thickness of the source rock is around 25 m (Wiesner 1983). In the Schoonebeek area, the Bentheim sequences form sandstone wedges that act as stratigraphical traps (Kockel et al. 1994). The Lower-Middle Cretaceous shales seal the Schoonebeek reservoir below that contains the migrated hydrocarbons from the lacustrine Berriasian succession.

Materials and methods

The material available for this study was obtained from three NAM cores in the Schoonebeek field, the cores 495, 586 and 590. During a one-week stay at the core storage of NAM at Assen (March 2001), depositional and diagenetic features of the Schoonebeek sandstones were analysed by means of sedimentological logging. Core plugs and samples were taken for further study. In addition, geophysical well logs (natural gamma radiation and electrical resistivity) and porosity-permeability data from core plugs were obtained.

The herein treated Schoonebeek drill cores 495, 586 and 590 were obtained from depths ranging from 1024 m to 739.4 m (the core 495: 1024-938 m, the core 586: 976-926.2 m and the core 590: 770.4-739.4 m).

From visual observations during the visit at NAM and with guidance of the core photographs, a sedimento-

Table 1. Methods and number of samples.

Method	Number of samples
Polarised light microscopy	43
SEM (BSE)	36
XRD	9
SEM-CL	2 Gildehaus (outcrop)
AAS	12
LECO	10
SEM (SEI)	7 (2 from outcrop)

(See Figs. 5 and 6 for location, analytical methods and sample number).

logical log was established for each core. From each facies a number of samples were selected for analyses and quantification of textures and detrital and diagenetic components.

The sandstones were described and analysed in detail using multiple analytical methods (Table 1). The results were used to assess the relationships between diagenesis, petrophysical properties and reservoir heterogeneity. Analytical methods used in this study include thin section polarised light microscopy (PPL), scanning electron microscopy (SEM-BSE-CL) on carbon coated polished "stubs" and polished thin sections, SEM secondary electron microscopy (SEM-SEI) on gold coated freshly fractured rock samples, backscattered electron image point counting (384 points per image), X-ray diffractometry (XRD) of whole rock samples and clay fraction subsamples, atomic absorption spectrophotometry (AAS), cathodoluminescence analysis (CL) of thin-sections and organic matter/carbonate content analysis (LECO).

Forty-three samples were selected from the cores for preparation of thin sections. Of these 32 were from permeable strata and the remaining 11 were from impermeable carbonate-cemented layers and carbonate nodules. However, the emphasis of the study was on the permeable sandstone samples. The carbonated-cemented and carbonate horizons were used complementary to describe early diagenesis and to assess its potential use for interwell correlation.

All thin sections were digitally photographed by means of polarisation microscopy as a complement to the BSE images. In addition, 36 polished "stubs" were prepared for scanning electron microscopy (SEM), 24 samples from the Bentheim Sandstone and the remaining 12 samples from the carbonate nodules. Material for both thin sections and the polished "stubs" were taken from the same core locations. Several BSE microphotographs were taken for analysis and quantification of detrital and diagenetic components in the "stubs". The petrographical and other analytical data from the cores were related to the burial history and early and late diagenesis of the Lower Saxony basin.

Scanning electron microscopy (SEM)

Backscatter electron imaging (BSE)

The method was used as a complement to conventional polarised microscope point counting. Carbon mounted polished "stubs" were analysed by means of the backscatter electron imaging (BSE). Trewin (1988) made a detailed description of this technique, in which the mineral densities were mapped and reproduced as a grey scale (white = heavy, black = light) due to differences in atomic weight. This approach was used for point counting of the images from the selected "stubs", which is more accurate than conventional point counting. The data were used to classify the arenites of the Schoonebeek cores in a QFL-diagram (see Pettijohn et al. 1972).

SEI secondary electron imaging

In this study, secondary electron imaging (SEI) of fractured samples was used to get three-dimensional overviews of the presence and distribution of the mineral phases and pores in the sample (cf. Trewin 1988). The main purpose for applying this method was to detect quartz cement. Freshly broken rock pieces were glued on specimen holders and sputtered with gold, and a carbon layer mounted on the side of the sample to achieve conductive contact between the specimen and the holder.

X-ray diffractometry

Nine samples were used for analyses of the mineralogy of the clay-size fraction (<2 micron fraction), using oriented samples. These nine samples represent different facies and depositional environments. The sandstones were gently disintegrated and subsequently the clay fraction was separated by means of gravity settling. The clay fractions were smeared (horizontally orientated) on glass slides and dried overnight at room temperature. Untreated (i.e. air-dried) slides were first analysed, by means of XRD. Five samples were analysed after being heated to 490 °C for two hours, and analysed again after being heated to 550°C for two hours. Multiples of these samples were also saturated with ethylene glycol prior to radiation, which makes identification of clay minerals with swelling properties such as smectite possible. The remaining four air-dried samples were only analysed after preheating to 550°C for two hours. The heating of samples was done to avoid the identification problems due to overlapping XRD-peaks. Hence, at 550°C chlorite tends to increase in intensity, whereas at 550°C kaolinite collapses (marked by disappearance of the 7 Angstrom reflection which kaolinite has in common with chlorite) while dickite remains stable. The heating up to 550°C therefore serves to control the composition of the kandites (kaolinite and dickite). Heating thus allows to distinguished kaolinite from chlorite, which also may have a main reflection at 7 Angstrom. Heating does not affect illite to collapse.

Whole rock chemical analysis (atomic absorption spectrophotometry)

The whole rock contents of K, Al, Mg and Ca were determined in 12 samples. The chemical analysis was done by means of atomic absorption spectrophotometry (AAS). The finely ground samples were fused with lithium metaborate in a platinum crucible and the melt of each sample was dissolved in dilute nitric acid with added caesi-

um-chloride. The result of the AAS depends on electron transitions between specific energy levels within the electron shells of the atoms in the solution. Each analysed element absorbs light at a characteristic set of wavelengths. The light was supplied from a cathode hollow lamp with precise wavelengths and the samples (solutions) were atomised by a flame. The instrument measures the reduction in the intensity (absorbency) of the characteristic wavelengths. All samples were calibrated to standards with known concentrations of the analysed element, and a number of standard solutions were made with different concentrations. The absorbency of each sample was measured and a linear correlation was calculated according to Beer's law. Accordingly, the absorption is proportional to the concentration of the free atoms in the vapour. Blank solutions were also run and the average values of these were subtracted from the measured values. By applying the given equation and to correlate with the sample weight, the appraisal to obtain element concentration in the solution was calculated, according to

$K_2O\%$= ((mg/ml *dilute factor)/sample weight)* total volume 100ml* 1/10000

Two samples were analysed for each rock sample and the results were averaged.

Cathodoluminescence microscopy

Thin sections from Gildehaus were analysed by means of cathodoluminescence (CL) both by using a cold cathodoluminoscope and a CL detector attached to a SEM. This was done after BSE examination. The cathodoluminescence device (the vacuum chamber and electron gun) was placed on the rotation table of a conventional transmitted polarised light microscope to achieve discrimination of detrital and authigenic quartz and for quantification of authigenic quartz cement. The electron bombardment of the thin sections causes the emission of visible light (cathodoluminescence). The visible CL reveals the diagenetic fabrics and the composition of detrital grains and cements (Miller 1988). The identification of detrital and authigenic quartz in CL is derived from differences in crystal lattice structures, where detrital quartz of igneous or metamorphic source has characteristic lattice imperfections (Owen 1991). Thus, the authigenic quartz cement shows a more perfect crystal lattice due to lower precipitation temperature and pressures than the detrital quartz has experienced, where detrital quartz has detectable intensities and authigenic quartz cement has reduced to non-luminescence appearances (Owen 1991). According to Budd et al. (2000) a number of trace elements incorporated within the mineral may quench luminescence or reduce luminescence intensity and influence the spectrum (change the luminescence colour). Authigenic quartz cements from the Gildehaus thin sections were photographed with CL and point-counted for the quantification of quartz cement. CL images from the Gildehaus samples were used to quantify quartz cements.

Organic matter and carbonate analyses (LECO)

The LECO analyses of ten samples were done for the quantification of bitumen and the discrimination between bitumen and clay matrix in the pore and fracture systems of the different facies.

The analytical instrument is a microprocessor-controlled device for the determination of carbon and sulphur. Ten samples were weighed before they were combusted in a high-frequency furnace. The products of combustion (ionised matter) passed trough either a sulphur IR-cell or a carbon IR-cell. Prior to the combustion of the samples, a calibration of carbon and sulphur was done. Finally, the results were adjusted for sample weight and the calibration factors.

Results

Description of cores

The following categories of rocks can be distinguished in the tree cores (Table 2):

Bioturbated sandstone
Massive sandstone
Heterolithic sandstone
Shale (in the Sch-495 core only)
Open marine sandstone
Carbonated-cemented layers and carbonate nodules (appear in the massive sand, the bioturbated sand and in the shale)

The Schoonebeek-495 core

The core consists of five different categories (Fig. 5), which are: (1) shale (25.4 m 3.8 m thick), (2) bioturbated sandstone (5.3 m and 10.3 m thick), (3) massive sandstone (3.7 m thick), (4) heterolithic sandstone (24.1 m thick) and (5) an iron-ooid containing, open marine sandstone (13 m thick). The sequence starts with shale, overlain by bioturbated sandstones that gradually change into more massive sandstone. The Schoonebeek-495 core continues with heterolithic sandstones and bioturbated sandstone. Shales overlay the sandstone and the succession

Table 2. Category description.

Categories	Present in core	Description – sedimentary structures
Bioturbated sandstone	495	Biogenic structures in flaser-bedded sandstone
Massive sandstone	590 & 586	Massive (debris flows or large-scale bedding structures)
Heterolithic sandstone	495	Rhythmic sand/silt alternation (0.02 m thick intervals)
Shale	495 & 586	Fissile claystone
Open marine sandstone	495	Reworked sandstone with ooids and pedogenic structures
Carbonate cemented layers	495, 590 & 586	Carbonate cement layers (0.3-0.5 m thick)
Carbonate cemented nodules	590 & 586	Carbonate cemented siliciclastic sand (0.1-0.2 m thick)

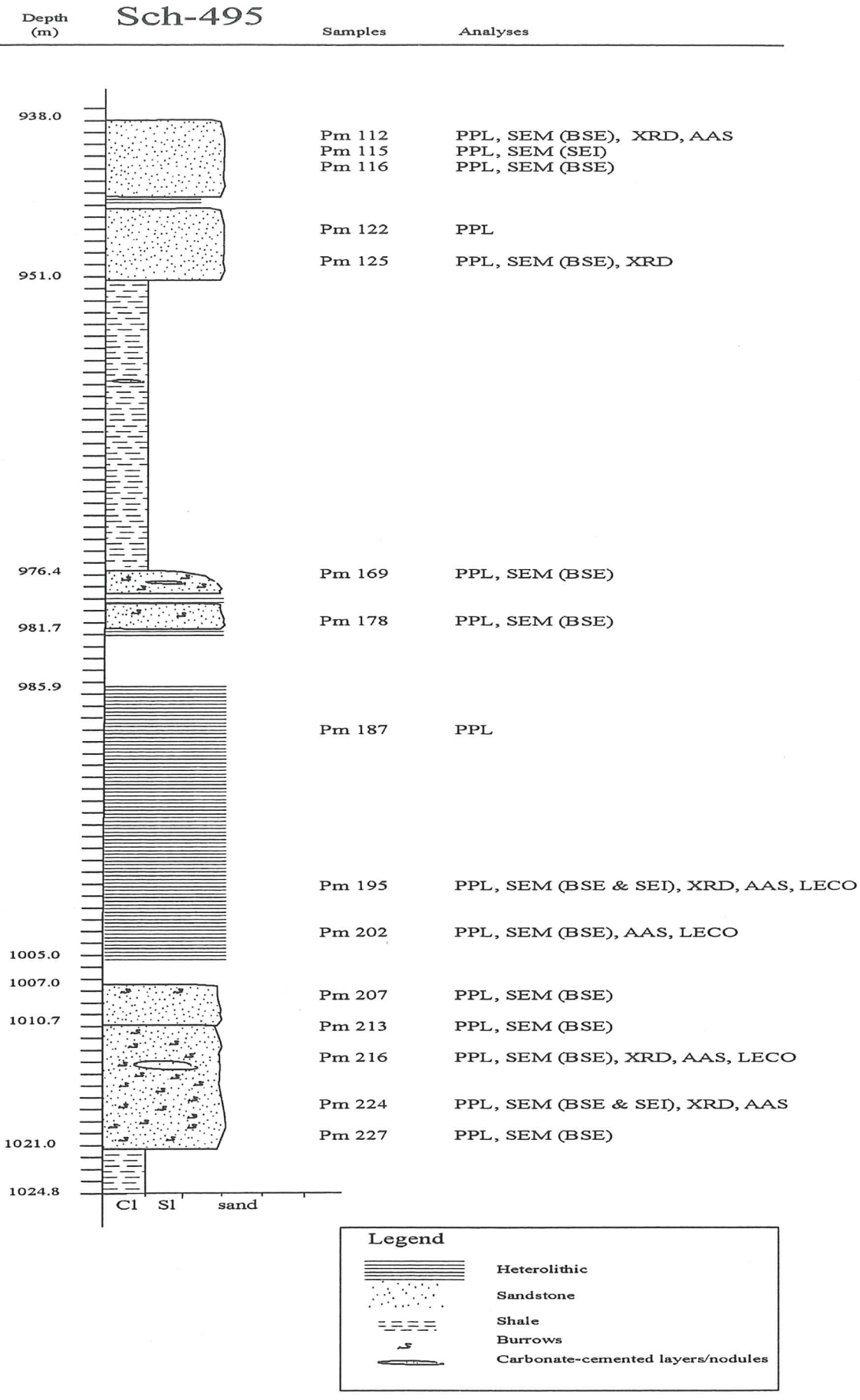

Fig. 5: The log of Sch-495 with locations and the results of analyses.

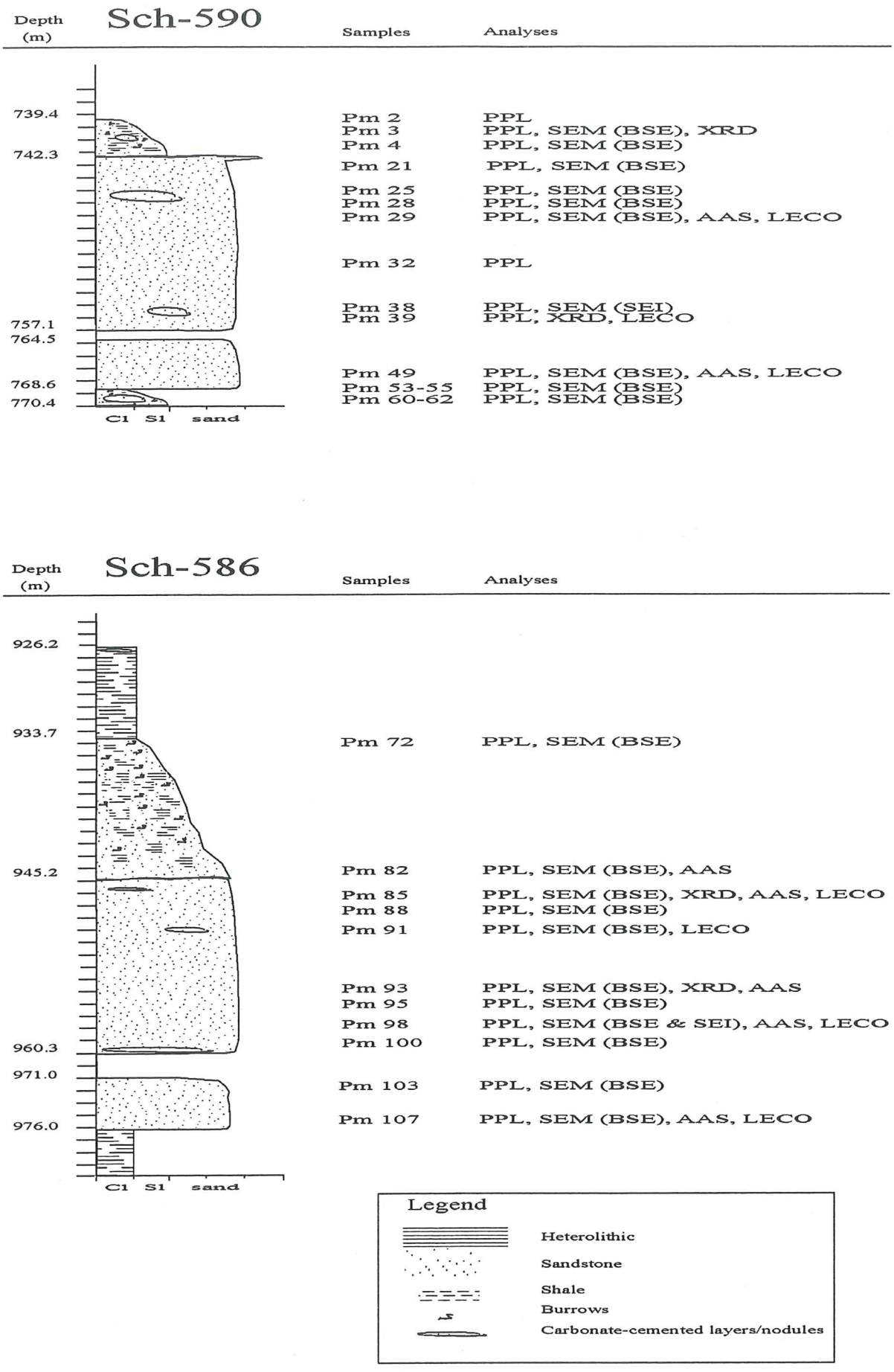

Fig. 6: The log of Sch-590 and 586 with locations and results of analyses.

ends with open marine sandstones. A number of carbonated-cemented horizons occur within the sandstones, both in the massive and in the bioturbated sandstone. Carbonate shells from bivalves were found in the shale.

The Schoonebeek-590 core

This core consists from the base and upwards of bioturbated sandstone (1.7 m thick), massive sandstone (4.1m thick) and after core loss (7.4 m) again, massive sandstone occurs (14.8 m thick) followed by bioturbated sandstone (2.8 m thick). Carbonate-cemented layers and carbonate nodules are present, both in the massive and bioturbated sandstones (Fig. 6).

The Schoonebeek-586 core

The succession in this core consists of four lithologies (Fig. 6). These are, from base: shale (5 m thick), massive sandstone (19,2 m thick) except from an 11.6 m gap (core loss) in the sandstone, bioturbated sandstone (11.5 m thick) with a gap of 8 m (core loss), and shale (7.5 m thick). The core shows a pattern similar to the Sch-590 core, with carbonate-cemented layers and carbonate nodules being present in the succession.

Petrographic analyses

The Schoonebeek cores

Bioturbated sandstone

The bioturbated facies is dominated by poorly sorted sand with a bimodal grain-size distribution. It is mainly medium to fine-grained and composed of subrounded quartz grains and a few percent of K-feldspar (Plate 1, Fig. 7). The quartz grains are of monocrystalline, undolous monocrystalline and polycrystalline type and show some sheared sutures. The pores of the bioturbated sandstone are primary intergranular and have partly been filled with detrital clay. Secondary pores are present in the bioturbated sandstone, as indicated by the occurrence of oversized pores. The appearance of micropores is restricted to the detrital clay and the partly dissolved K-feldspars. The detrital clay minerals are composed of kaolinite and illite. The concentration of pyrite is fairly high in some samples and pyrite is a common constituent throughout the facies. Calcite is present as authigenic material.

Massive sandstone

The massive sandstones are composed of well-sorted, coarse-grained sand. The quartz grains are angular to subrounded, and include quartz types such as monocrystalline, undolous monocrystalline and polycrystalline, occasionally with sheared sutures (Plate 1, Fig. 8). Corroded edges of quartz grains are present, (Plate 1, Fig. 9). In some samples, the grain-size distribution shows a slight bimodality, and the larger quartz grains show the most rounded grains textural inversion. The K-feldspar content is just a few percent. The massive sandstone has an excellent primary intergranular porosity, where only a low content of detrital clay (kaolinite and illite) fills the pore space. A significant portion of the pores is of secondary origin, showing two distinct pore sizes, i.e., both regular (matching the adjacent K-feldspar grains) and oversized pores.

Heterolithic sandstone

The heterolithic sandstone is very similar to the massive sandstone in its content of quartz types. The medium-grained sandstone is moderately well sorted and composed mainly of subrounded quartz grains (Plate 1, Fig. 10). The primary intergranular pores in the heterolithic sandstone have been partly filled with detrital clay, whereas the silty intervals are almost impermeable. The amount of secondary pores is low, where the pore size reflects the dissolution of K-feldspar. Micropores are concentrated to the detrital clay and to the partly dissolved K-feldspars. The heterolithic sandstone has a lower percentage of K-feldspar than the massive sandstone. Because of the finer-grained interlaminations, the content of detrital clay (kaolinite and illite) is higher than in the massive sandstone. Concentrations of glauconite grains and precipitates of authigenic calcite are also recorded in this facies.

Open marine sandstone

This category is different from the other sandstones. The open marine sandstone contains abundant iron-ooids and a matrix-supported framework (Plate 1, Fig. 11). The open marine sandstone facies is poorly sorted, and has a matrix of chlorite and calcite with iron ooids and an increase in quartz grain size compared to the other categories. Subrounded quartz grains predominately include monocrystalline, undolous monocrystalline and polycrystalline grains with sheared sutures. The K-feldspar content is very low and there are no intergranular pores present. The intergranular volume is filled with detrital clay or calcite cement. The porosity existing is adjacent to iron-ooids and as micro pores within the detrital clays. In the matrix, there are large amounts of glauconite. Siderite, shell fragments and silt particles are also present.

Carbonate-cemented layers and carbonate nodules

The pore filling carbonate-cement has preserved the open framework textures (high IGV; intergranular volume) (Plate 2, Fig. 12). Iron ooids with concentric interval lamination and siderite nodules are observed in the carbonate nodules in the core Sch-590. The carbonate-cemented layers in the massive sandstone of the core Sch-590 show normally graded lamina with gastropods in the calcite cement, but large bioclasts also occur in the nodules. The bioclasts in the carbonate-cemented layers and in the nodules often show a neomorphism.

Sandstone composition

The composition of the sandstone, its texture, sorting, content of feldspar, mica and concentration of clay are all parameters that are reflected in the porosity and permeability. The compositions of the sandstones have been determined by point counting of SEM-BSE images (Table 3) The Bentheim Sandstone is predominantly quartz arenites according to the classification of Pettijohn et al. (1972) with an average composition of $Q_{96.2}F_{3.8}L_0$ (Fig. 13). The quartz grains are composed of monocrystalline

Table 3. Results of point- counting of BSE images in percentages (%).

Sample number	Quartz	K-feldspar	Mud matrix	Siderite	Pyrite	Iron-ooids	Porosity	Other
Sch-590								
Pm 21	56.96	1.80	1.55				39.69	
Pm 29	49.49	2.03	1.01				47.21	0.26
Pm 49	42.45	2.08	36.98		2.43		15.63	0.43
Sch-586								
Pm 82	59.63	1.04	1.56		0.52		36.72	0.53
Pm 85	57.89	0.75	1.25		1.00		38.85	0.26
Pm 88	61.62	0.26	1.31		0.52		35.77	0.52
Pm 91	54.17	1.83	0.78				43.22	
Pm 93	59.53	2.87	1.83				35.77	
Pm 95	41.99	1.58	0.79				55.64	
Pm 98	63.45	3.13	5.22		0.26		26.89	1.05
Pm 100	46.09	1.04	0.52		0.79		51.56	
Pm 103	59.48	3.38	0.26		0.78		36.10	
Pm 107	65.28	3.37	3.89				27.20	0.26
Sch-495								
Pm 112	49.21		27.75	8.64		7.07	5.76	1.57
Pm 125	49.11		33.84	3.42			13.22	0.51
Pm 169	14.12		14.67		54.03		17.18	
Pm 178	58.16	2.08	14.55		4.94		20.26	
Pm 195	57.55	2.35	11.46		0.78		27.86	
Pm 202	58.79	0.96	15.65		0.96		22.68	0.96
Pm 207	67.19	2.62	8.14		0.52		18.37	3.16
Pm 213	50.00	3.93	27.74				17.80	0.53
Pm 216	24.48	1.82	68.75				4.43	0.52
Pm 224	48.38	3.78	25.94				21.62	0.38
Pm 227	37.08	0.30	6.08					0.61

quartz, (undulous) monocrystalline quartz and polycrystalline quartz. The shape of the quartz grains is mostly angular to subrounded with abundant corroded margins. With increasing grain size the shape of the quartz grains are more rounded (which was observed from sandstone samples with bimodal grain size distribution). The K-feldspar grains have well-developed cleavage and some show clearly a microcline type of twinning. The K-feldspar grains are often elongated and angular in shape due to breakage along cleavage planes during sedimentary transport. Most of these grains show evidence of limited dissolution, preferentially along the cleavage planes and twin boundaries (Plate 2, Fig. 14). The oil/bitumen occurs in the massive, bioturbated and heterolithic sandstone, whereas detrital clay is abundant in the open-marine, the bioturbated and the heterolithic sandstone. Calcite cement is abundant throughout the Bentheim Sandstone, whereas quartz cement was not observed in the investigated cores. Glauconite grains have been developed in all of the three cores and facies. Iron ooids were formed in the open-marine sand and the Sch-495 core, but were also sparsely found in bioturbated sandstone in core Sch-586. A bimodal grain-size distribution is common in the bioturbated and open-marine sandstone in Sch-495 and Sch-586, but was also present in parts of the massive sandstone in the Sch-590. Authigenic pyrite and siderite was locally present in pores, but in sample Pm 169 pyrite almost dominates the pore space. The presence of siderite is restricted to the open marine sandstone and to the carbonate cemented nodules, which indicate precipitation after the sediment subsided throughout the sulphur reduction zone.

Petrophysical data provided by NAM

The porosity and permeability results generally show that the bioturbated sandstones have very variable porosities and low permeabilities, whereas the massive sandstones have the highest porosity and permeability (Table 4 and Fig. 15). The heterolithic sandstone shows variable permeability values, whereas the porosities are high in the sand intervals and low in the silty intervals. The open marine sandstone has fairly high porosity and very low permeability.

In Table 5 a correlation was made between NAM porosity and point-counted porosity to estimate the effect

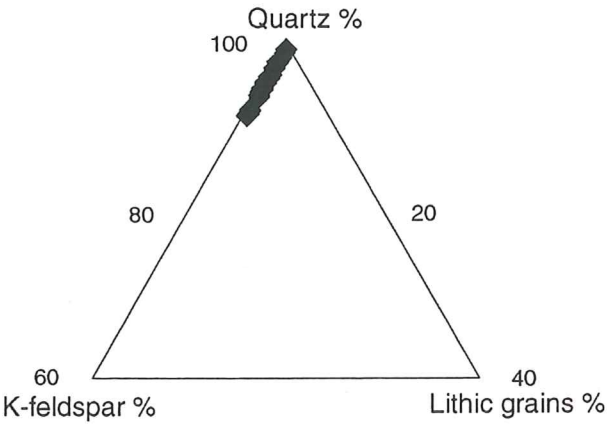

Fig. 13. QFL-triangle with the present day detrital composition of the Bentheim Sandstone. Although the sandstones are quartz arenites (according to the classification system of Pettijohn et al. 1972), they probably originally contained more feldspar (prior to dissolution during burial) and had an original subarkosic to arkosic composition.

Table 4. Relationship between depositional categories and the main petrophysical properties provided by NAM (the average porosity and permeability).

Category	No	Porosity (%)	Standard deviation	Permeability (mD)	Standard deviation
Massive	72	33.41	3.19	3259.93	1901.67
Bioturbated	12	23.52	10.10	129.90	217.75
Heterolithic	42	29.25	6.71	1901.87	2056.64
Open marine	36	30.89	4.10	5.05	8.31
Gildehaus	12	23.87	1.51	1350.33	604.73

of secondary porosity and microporosity in the samples. The petrophysical properties can be assigned to the depositional environment. The distribution of secondary pores and micro pores was related to the provided NAM petrophysical properties.

Secondary porosity

Estimations of secondary porosity in the massive sandstone were conducted in order to estimate its effect on petrophysical properties (Table 6 and Fig. 16).

Clay mineralogy

The mineralogical composition of the clay-sized fraction has been determined using XRD from samples Pm 4 (carbonated-cemented nodule), Pm 39, 85, 93 (massive sandstone), Pm 112, 125 (open marine sandstone), Pm 195 (heterolithic sandstone) and Pm 216, 224 (bioturbated sandstone). Pm 4 and Pm 39 are from Sch-590, Pm 85 and Pm 93 from the Sch-586, whereas Pm 112, 125, 195, 216 and 224 are from Sch-495 (Fig. 17, see also appendix). Kaolinite and illite are the two dominant clay minerals in the massive, bioturbated and heterolithic sandstones, whereas in the open marine sandstone, kaolinite and illite are rare (Table 7).

AAS

The AAS analysis was done in order to correlate Al and K, Mg and Ca, Mg and Al, and calculate calcite from the Ca content. The approach for the correlation was to make an appraisal of the elements Al, Mg and K capacity to bind to clays. The massive sandstone has Al-contents around 0.20-0.30 %, except from Pm 49, whereas the Al- content of the heterolithic sandstone is slightly higher (0.28-0.50%) (Table 8). The highest concentration of Al is found in the open marine and the bioturbated category. The bioturbated sandstone has the highest potassium concentration (2.20-1.00%), whereas the massive and

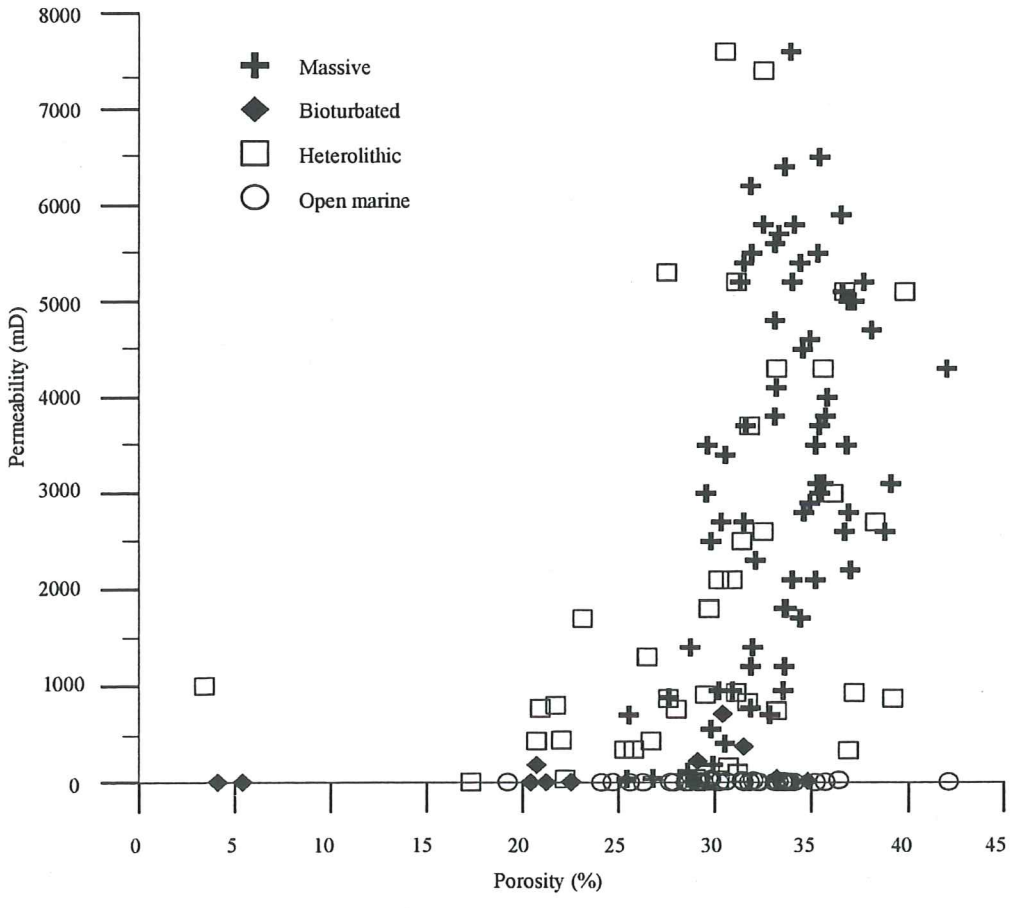

Fig. 15. The porosity and permeability in the four sandstones in Schoonebeek field. The bioturbated and open marine sandstone have by far the lowest porosities and permeabilities. NAM provided the petrophysical data.

Table 5. Point-counted porosity, and mud matrix content compared to porosity, permeability and grain density provided by NAM.

Samples	Helium Porosity (%)	Porosity (p-counted) %	Mud matrix (p-counted) %	Secondary porosity	Micro porosity	Grain density (g/cm²)	Permeability (mD)	Sandstone
Sch-590								
Pm 21	23.10	39.69	1.55	Medium		2.644	120.00	Massive
Pm 29	25.54	47.21	1.01	High		2.642	700.00	Massive
Pm 49	26.81	15.63	36.98	Low		2.649	38.00	Massive
Sch-586								
Pm 82	29.80	36.72	1.56	High		2.650	2500.00	Massive
Pm 85	31.30	38.85	1.25	Medium		2.650	5200.00	Massive
Pm 88	32.50	35.77	1.31	High		2.640	5800.00	Massive
Pm 91	34.00	43.22	0.78	High		2.650	2100.00	Massive
Pm 93	31.60	35.77	1.83	Medium		2.650	3700.00	Massive
Pm 95	35.20	55.64	0.79	Very high		2.650	3500.00	Massive
Pm 98	32.10	26.89	5.22	Medium		2.650	2300.00	Massive
Pm 100	38.10	51.56	0.79	High		2.640	4700.00	Massive
Pm 103	42.00	36.10	0.26	Medium		2.660	4300.00	Massive
Pm 107	30.20	27.20	3.89	High		2.650	950.00	Massive
Sch-495								
Pm 112	33.10	5.76	27.75		Very high	2.870	1.80	Open marine
Pm 125	27.70	13.22	33.84		Very high	2.710	2.50	Open marine
Pm 169	20.40	17.18	14.67			2.720	0.84	Bioturbated
Pm 178	33.20	20.26	14.55	Low		2.690	43.00	Heterolithic
Pm 195	36.90	27.86	11.46	Medium		2.640	3300.00	Heterolithic
Pm 202	25.80	22.86	15.65	Low		2.620	340.00	Heterolithic
Pm 207	32.50	18.37	8.14	Medium		2.650	2600.00	Bioturbated
Pm 213	34.50	17.80	27.74	Low		2.650	780.00	Bioturbated
Pm 216	26.20	4.43	68.75	Low	High	2.760	0.09	Bioturbated
Pm 224	33.00	21.62	25.94	Low	High	2.650	160.00	Bioturbated
Pm 227	34.00		6.08			2.680	140.00	Bioturbated

heterolithic sandstones have lower contents in the same range (0.80-0.30%). Pm 49 differs with higher content (1.25%) than the other samples of the massive sandstone. The open marine sandstone has the lowest content of Al of all investigated samples in the analysis.

The Mg contents of the massive and the heterolithic sandstones are more or less comparable, whereas the Mg content of the heterolithic sandstone is slightly higher. Sample Pm 49 differs from the rest of the measured samples from these facies. The bioturbated sandstones have higher Mg-content than the massive and heterolithic facies. The highest Mg-contents are found in the open marine sandstone. Ca analysis did not reveal any significant concentration differences. However, the highest content of calcite is observed in the open marine sandstone (Table 9).

Table 6. Secondary porosity in percent of total porosity of the massive sandstone.

Sample	Secondary porosity (%)
Pm 21	22.08
Pm 29	29.49
Pm 49	5.00
Pm 82	29.08
Pm 85	14.84
Pm 88	25.55
Pm 91	27.71
Pm 93	21.90
Pm 95	50.99
Pm 98	17.48
Pm 100	36.36
Pm 103	15.11
Pm 107	30.48

Fig 18 displays element cross-plots of whole rock samples by means of bound the elements to clays. AL and K correlate slightly positively R=0.7497 and the correlation does not improve considerably if Pm 112 and Pm 216 are disregarded. The B and C plots show no correlation, where sample Pm 112 and Pm 216 differentiate from the average composition of the measured ions. Plot D correlates slightly positively if Pm 112 and Pm 216 are disregarded. Pm 112 was obtained from the open marine

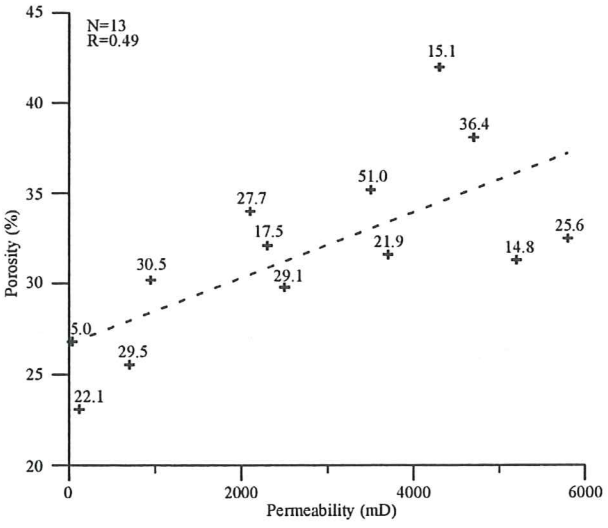

Fig. 16. Porosity versus permeability plot of the massive sandstone samples and the effect of secondary porosity on porosity and permeability. The percentage contents of the secondary porosity noted above the plot marks (the secondary pores content in percent of total amount of porosity).

Table 7. Results from XRD on oriented on the clay fraction samples. Estimations of the clay fraction content (low = + and high = +++).

Sample	Kaolinite	Illite
Pm 3	+	+
Pm 39	+	+
Pm 85	+	+
Pm 93	+	+
Pm 112	+	+
Pm 125	+	
Pm 195	+	
Pm 216	+++	++
Pm 224	+++	+++

Table 8. The result of AAS (average from two analyses of each sample).

Sample	Al%	K%	Mg%	Ca%
Pm 29	0.2700	0.8390	0.03875	0.0379
Pm 49	1.3164	1.2560	0.1795	0.1590
Pm 82	0.2058	0.5975	0.0376	0.0822
Pm 85	0.2385	0.8135	0.0347	0.0870
Pm 93	0.2917	0.6125	0.0504	0.1759
Pm 98	0.2670	0.5910	0.0480	0.0979
Pm 107	0.2395	0.5595	0.0451	0.0772
Pm 112	1.7060	0.3530	2.8166	3.1659
Pm 195	0.2775	0.6040	0.0679	0.2055
Pm 202	0.4814	0.7725	0.0922	0.3108
Pm 216	6.4678	2.2075	0.6408	0.4504
Pm 224	1.09605	1.0195	0.1550	0.1224

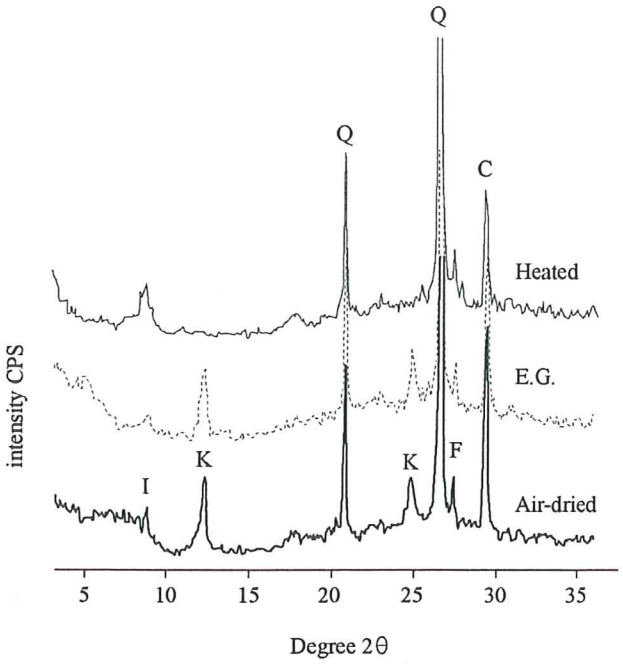

Fig. 17. Clay fraction XRD on sample Pm 85. The conducted XRD analyses, air dried (thick line), ethylene glycolated (dotted line) and heated 550ºC (thin line). A low content of kaolinite and illite is present as detrital clay in the sample, where also calcite cement occurs. Quartz dominates the sample. The components of the diffractograms include detrital illite (I), and kaolinite (K), quartz (Q), K-feldspar (F) and authigenic calcite (C).

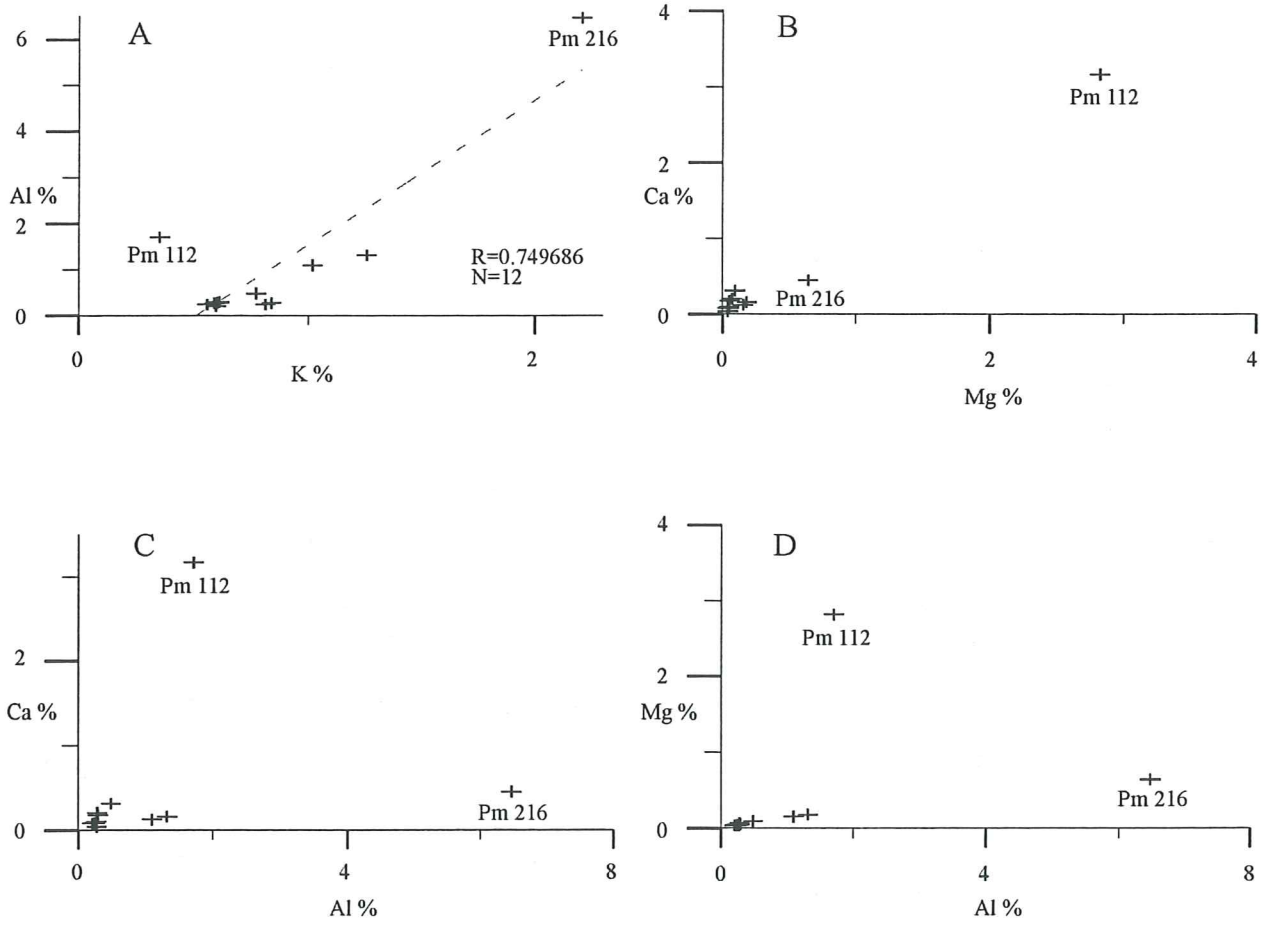

Fig. 18. Cross-plots A-D of 12 samples from the subcrop. Pm 112 and Pm 216 are the labelled samples, due to their difference from the other samples in element concentration.

Table 9: The calcium carbonate content in percent.

Sample	Carbonate content %
Pm 29	0.0152
Pm 49	0.0637
Pm 82	0.0329
Pm 85	0.0348
Pm 93	0.0704
Pm 98	0.0392
Pm 107	0.0309
Pm 112	1.2664
Pm 195	0.0822
Pm 202	0.1243
Pm 216	0.1802
Pm 224	0.0490

sandstone, which has no similarity with the other categories and the sandstone consists of high content of Al, Mg and Ca (see Table 8 and 9). Pm 216 has the highest content of mud matrix and the lowest content of quartz grains of all the bioturbated samples that were taken from the bioturbated sandstone (see Table 3).

LECO total organic carbon

The total carbon content (carbon from organic matter and carbonates) was analysed in order to quantify bitumen and to discriminate bitumen from clay matrix in the pore and fracture systems of the different categories. The data confirms that bitumen was present in the massive, heterolithic and bioturbated sandstone samples in all three cores (Table 10). Sample Pm 91 has a negligible carbon content compared to the other massive sandstone samples. The bioturbated sandstones have lower carbon content than the massive and heterolithic sandstone. Exceptions were observed in samples Pm 91 and Pm 107, which show lower carbon contents than the bioturbated sandstones.

Petrography of the Bentheim sandstone in Schoonebeek and Gildehaus

The sandstone composition of samples from Schoonebeek (subcrop) and Gildehaus (outcrop) are similar (Gildehaus material from Mansurbeg 2001). Both have a content of quartz grains that are composed of monocrystalline quartz, (undulous) and polycrystalline quartz. K-feldspar dominates the feldspar population in both subcrop and outcrop. Samples from the Gildehaus outcrop include massive and cross-bedded sandstones. In the Schoonebeek cores detrital clay (kaolinite and illite) is present, whereas in Gildehaus outcrop material detrital clay is absent. Clay materials are present as authigenic clay (kaolinite-dickite). The Bentheim successions in Schoonebeek and Gildehaus contain primary intergranular pores (depositional pores), as well as micropores and moldic pores (oversized pores). The difference between the Gildehaus and the Schoonebeek successions is that the outcrop samples have reduced intergranular pores that are partly filled

Table 10. LECO analysis with carbon and sulphur content. The sulphur content cannot be correlated with the point-counted pyrite content from the BSE-photographs. The sulphur content instead reflects the sulphur in the oil/bitumen that is present in the samples.

Sample	Carbon (%)	Sulphur (%)
Pm 29	8.563	0.1687
Pm 39	6.834	0.3464
Pm 49	4.538	0.5947
Pm 85	6.219	2.137
Pm 91	0.1975	0.0313
Pm 98	2.251	0.4066
Pm 107	0.9770	0.5381
Pm 195	2.634	0.3253
Pm 202	1.861	0.3670
Pm 216	1.381	0.2878

with quartz overgrowths, whereas in the subcrop samples quartz cementation is absent. Moreover, in the Gildehaus samples authigenic kaolinite-dickite is common, filling primary pores and oversized pores. There is abundant moldic pores (secondary pores) both regular (matching the adjacent grains) and oversized in both outcrop and subcrop, whereas the occurrence of moldic pores both formed by dissolved K-feldspar and bioclasts are higher in the Schoonebeek samples. These petrographical differences can also be seen in the petrophysical properties, where the Gildehaus samples have generally lower permeability and slightly lower porosity values than Schoonebeek samples (Fig. 19).

The petrography of the Bentheim Sandstone in the Bramberge area is comparable. The major minerals present according to Grote-Sedlacek (1984) are K-feldspar, calcite, dolomite, siderite and pyrite. The clay minerals primarily include, kaolinite, illite, chlorite and mixed illite-montmorillonite were present (Grote-Sedlacek 1984).

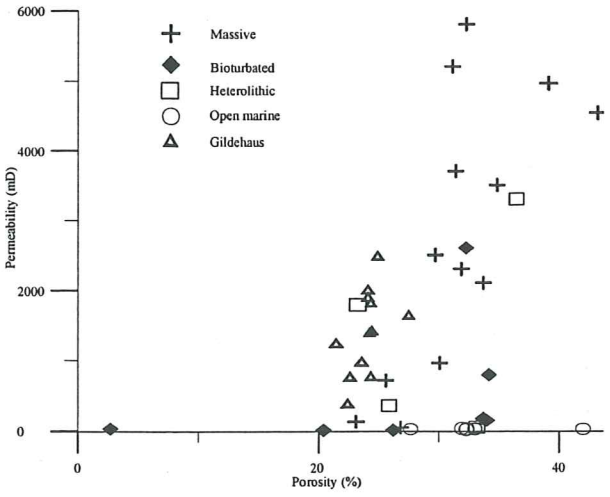

Fig. 19. The petrophysical properties of Schoonebeek and Gildehaus samples. The Gildehaus samples were taken from massive sandstone (thick beds with large-scale cross bedding) or subaqueous dunes (thinner sandstones with clearly visible cross bedding). The quartz cementation in Gildehaus has reduced the intergranular pores and hence decreased the petrophysical properties in the outcrop. The open marine sandstone has no similar facies in the Gildehaus samples and therefore no comparison can be made (cf. Mansurbeg, H. 2001).

Interpretations

Depositional environment

The rate of deposition in shallow-marine settings is a function of the ability of the adjacent land areas to provide a clastic sediment supply, of accommodation space, and of lateral marine sediment reworking. In addition, tidal currents, waves and near shore currents rework the coastal sediments and distribute sediments. The subsidence rate and the amount of accommodation space maintained are other factors that affect the thickness of the preserved sand facies. In addition, large-scale forces such as those induced by tectonic activity and relative sea level changes affect the depositional system and control its geographical extent and the geometry of the sand bodies. The Bentheim Sandstone succession is a shallow marine sandstone unit that reflects a near shore environment. Tidal processes dominated throughout the deposition of the Bentheim Sandstone (Mutterlose & Bornemann 2000). Wonham et al. (1997) claimed that the Bentheim Sandstone consists of several tabular sandstone bodies. Accordingly, the deposition of the Bentheim succession occurred between the early Valanginian and the beginning of late Valanginian, i.e., <1 Ma according to the chronostratigraphy of Gradstein et al. (1994).

The Schoonebeek cores can be correlated with the new stratigraphical division made by Mutterlose & Bornemann 2000 (see Fig. 3). The bioturbated sandstones of the Bentheim Sandstone formation are recognised as a flaser-bedded sandstones, in which thin mud drapes have been mixed into the sandstone by intense bioturbation (Wonham et al. 1997). This sandstone was deposited in estuarine environments (Wonham et al. 1997), as indicted by the abundant trace fossils and pyrite, in the Schoonebeek's cores (495, 586 and 590). In the massive sandstones (two different massive sandstones), the deposition environment of the Sch-495, 586 and 590 cores is more difficult to determine and can be the result of numerous gravity flow processes (marine turbidity or sandy debris flow) (Wonham et al. 1997). Alternatively, the internal structures may be too large to be recognised. Tentatively, the sands were quickly deposited without much grain size fractionation, which obscured internal cross bedding. The massive sandstones are assumed to be turbiditic or believed to be of barrier sand origin, which is presumed to have been deposited by coast parallel currents (Mutterlose & Bornemann 2000). The heterolithic sandstone pattern in the Sch-495 core indicates a deposition in a tidal environment, which is seen as rhythmic silt-mud and well-sorted sand depositions. This sandstone was deposited on structural highs during low-energy conditions (Mutterlose & Bornemann 2000). The open marine sandstone reflects deposition in a marine environment, which was starved with respect to sediment input, as implied by the high concentration of glauconite in core Sch-495. The precipitation of siderite also reflects reducing conditions within the sediment in core Sch-495, where the depositional environment resulted in low permeabilities due to clay laminae, or matrix, and high organic matter contents (Stonecipher 1999). Structures in the open marine sandstone show that several phases of reworking have affected the sandstone. The great abundance of iron-ooids in this sediment is either originally formed in an aquatic realm or is composed of pedogenic carbonate (Heikoop et al. 1996). The open marine sandstone has the appearance of a matrix-supported sandstone and the limited sorting of the sediment confirms that it was deposited in low energy environments. The shale in all Schoonebeek cores was developed during offshore setting of clay, e.g., during transgressive phases.

The Bentheim succession is a series of facies that pass gradually from one into the other. Most of these facies successions are bounded at the top and base by an erosional unconformity (Reading & Levell 1996). The distinguished categories of the Schoonebeek cores can be correlated to the new stratigraphical division (see Fig. 3). The base of the Bentheim succession in the three cores is bound by the *Platylenticeras* Clay of early Lower Valanginian age. The shale that is sharply overlain by the open marine sandstone in the Sch-495 core divides the Bentheim sequence into the Lower Bentheim and the Upper Bentheim Sandstone. The Upper Bentheim Sandstone and the Bentheim Sandstone succession is bound on the top with the *erectum* Clay of early Upper Valanginian age but this contact cannot be seen in Sch-495 core. The shale that overlays the bioturbated sandstone in the Sch-586 is presumed to be equivalent with the shale that divides the Lower Bentheim Sandstone with the Upper Bentheim Sandstone in the Sch-495.

The Bentheim succession indicates a change in the relative sea level, which can be seen as a general transgressive stage in the area, i.e., a marine intrusion entering from the southern North Sea. This starts with the deposition of the bioturbated sandstones, which indicates that the depositional system more likely prograded out to a marine environment (open marine sandstone) rather than retrograded to a fluvial or brackish environment. The Bentheim marine sequences are deposited on structural highs (anticlines) in a depositional system including subtidal delta mouth bars and estuary mouth shoals (Wonham et al. 1997). Walther's law (1894) has been used to explain that facies occurring in vertical contact with each other must be the product of spatially neighbouring environments and that facies occurring in a succession conformably above one another also have been formed in laterally adjacent environments (Reading & Levell 1996). This principle can explain that the investigated system has migrated basinwards and resulted in a formation of sandier-upward facies associations composed of heterolithic sandstone in the lower part and massive or large cross-bedded sandstones in the upper part. In this context the sand deposition stage ends with the deposition of the open marine sandstone. The deposition of mud increases, which is indicated by the deposition of the *erectum* Clay.

Grote-Sedlacek (1984) refers to the Bentheim Sandstone as coastal deposits, where the thickness of the sediment pile is related to the energy of the long shore currents. Betz et al. (1987) interprets the Valanginian depo-

sition of the Bentheim Sandstone as deltaic and inter shoreline sands along the basins margins. The carbonate-cemented layers or carbonate nodules that are found in the Bentheim sequences are presumed to indirectly indicate condensed horizons in the depositional system (Wonham et al. 1997). These carbonates are probably stratabound, but cannot be traced and correlated over wider areas (Grote-Sedlacek 1984).

A modern equivalent to the Bentheim Sandstone depositional environment would correspond to a tidally dominated coast with local delta lobe progradation interrupted by transgressions, where fluvial sediments being absent.

Correlation of the Schoonebeek cores with distribution and facies pattern of the Emsland area

In summery the three cores can be correlated with the new stratigraphical subdivisions, by Wonham (1997) and Mutterlose & Bornemann (2000) (Fig. 3; and Table 11). Mutterlose & Bornemann (2000) distinguished two different massive sandstones, the Basisbank and the Haupt sandstone. Most certainly, the massive sandstone in the Sch-495 core corresponds to the Basisbank.

Schoonebeek-495

The bioturbated sandstone and the overlying massive sandstone at the base of the investigated core segment may correspond to the sequence stratigraphical Bentheim 1 unit (see Table 11). The heterolithic sandstone can be related to depositions on structural highs and corresponds to the lower Bentheim 2 unit. The bioturbated sandstone on top of the heterolithic facies is also related to the Bentheim 2 unit and represents the transition between the heterolithic sandstone and the upper massive Haupt sandstone (Bentheim 2). This bioturbated sandstone has signs of tidal activity, including heterolithic stratification. The Bentheim 1 and 2 Sandstone represents the Lower Bentheim Sandstone, which is overlain by 20 m of shale. This shale can be correlated to the Romberg clay, which is poorly exposed but can be observed in the western part of the LSB (Romberg Quarry) according to Wonham et al. (1997). The core ends with the open marine sandstone, which is related to the Upper Bentheim Sandstone (Bentheim 3).

Schoonebeek-586

This core commences with a thin bioturbated sandstone equivalent to the lower bioturbated zone of Bentheim 1. This unit is followed by a massive sandstone, which correspond to Bentheim 1 or Bentheim 2. The sandstone dominates the core except for at the upper part where the sandstone is more bioturbated.

Table 11. Stratigraphic divisions made first by Wonham et al. (1997) and later by Mutterlose & Bornemann (2000).

Open marine sandstone	Bentheim 3
Shale in the Sch-495 core	Bentheim 3
Heterolithic sandstone	Bentheim 2
Massive sandstone	Bentheim 1 and 2
Bioturbated sandstone	Bentheim 1

Schoonebeek-590

A massive sandstone (Bentheim 1 or Bentheim 2) dominates the base of this core segment and is overlain by a thin bioturbated sandstone.

Heterogeneity of the reservoir

The heterogeneity of the reservoir properties corresponds to the occurrence of carbonate-cemented layers and nodules and the variability in porosity and permeability. This, in turn, can be related to changes in the depositional environment and to the variability in facies of the Schoonebeek cores. The transition from the *Platylenticeras* Clay to bioturbated sandstone (Bentheim 1) in core Sch-495 indicates a sequence boundary (cf. Mutterlose & Bornemann 2000). The petrophysical properties are related to the depositional features of the upwards-sandier facies associations in the sequence stratigraphical divisions Bentheim 1 and Bentheim 2. These are composed of bioturbated sandstone and heterolithic sandstone in the lower part and massive or large cross-bedded sandstone in the upper part of Bentheim 1 and 2. The trend shows the porosity and permeability are higher in the massive sandstones compared to the bioturbated and heterolithic sandstones. The overlying shale in the core Sch-495 divides the Lower Bentheim from the Upper Bentheim Sandstone. The shale has therefore a negative effect on the reservoir quality. The open marine sandstone overlays the shale and differs from the other sandstones in the Bentheim succession in terms of petrophysical properties (high porosity and very low permeability). According to Mutterlose & Bornemann (2000) the transition between the two upwards, sandier facies, i.e., the base of the shale and the uppermost part of the open marine sandstone, corresponds to a flooding surface. This directly controls the spatial porosity and permeability distribution.

The Bentheim Sandstone reservoir geometry consists of several sheet-like sediment bodies, which constitute stratigraphical traps (Wonham et al. 1997). Accordingly, the sand bodies are wedging out into interfingering muddier facies.

Diagenetic processes

Scherer (1987) listed the most important parameters that influence primary porosity during sandstone diagenesis. These include compaction (through grain rearrangement, plastic deformation, pressure dissolution, and brittle fracturing), authigenesis of minerals (the most important being cementation, which is also operating at near-surface conditions) and leaching. Tucker (1991) suggested that these diagenetic processes are controlled by factors such as the depositional environment, sediment composition and texture, pore-water chemistry and the depth of burial and timing of uplift. Cementation of sandstones is at least partly controlled by re-equilibration of the depo-

sitional mineralogy of the detrital components to the changes in chemical and physical conditions, thus the increasing pressure and temperature with burial depth (Aagaard et al. 1990). The two main cementation processes in sandstones are precipitation of silica and carbonate cements. The main sources of ions for carbonate cement in marine sandstones are derived from seawater, HCO_3^- from kerogen maturation and the dissolution of biogenic carbonates and carbonate intraclasts (Worden 1998). At great burial depth, both pressure dissolution and the reactions between silicate minerals may provide the silica necessary for precipitation of quartz cement. Silica is also released because of feldspar leaching during meteoric water infiltration (Bjørlykke & Egeberg 1993), although very little of that silica will be precipitated due to low temperatures and continued removal of released silica by precipitation of other authigenic minerals competing with quartz cement precipitation (Bjørlykke & Egeberg 1993).

The framework mineralogy of the Bentheim Sandstone changed to some extent with increasing burial depth. However, diagenesis appears not primarily to have been related to the increase in burial depth and increase in temperature, but seems merely to be the result of circulation of acidic fluids probably derived from hydrocarbon maturation. During this, the main change was the partial leaching of K-feldspar and leaching of most of the carbonate fragments and the consequent development of secondary pores (Molenaar personal comments 2002). The different reservoir changing processes in the Bentheim Sandstone, described below in detail, are:

- introduction of clay matrix,
- development of glauconite grains and iron ooids,
- precipitation of pyrite and siderite,
- precipitation of calcite and chlorite cement,
- development of secondary pores and the introduction of oil and bitumen (Fig. 20).

The introduction of clay is derived from depositional processes, whereas the precipitation of pyrite and siderite indirectly reflect the chemical conditions in the depositional environment. Ryan et al. (1997) suggest that the abundance of detrital carbonate has favoured the precipitation of ferroan carbonate rather than ferroan clay and this scenario can be observed in the open marine facies, where the only occurrence of siderite and the highest content of detrital carbonate are present in the investigated Bentheim Sandstone. Glauconite is formed between the boundary the oxic-anoxic zone, whereas pyrite and siderite typically form later in the anoxic zone below. Calcite cement occurs in two phases and the early cement has often resulted in stabilisation of the grain framework in the Schoonebeek field. Although calcite cementation was derived from local biogenic carbonate grains and diffusional redistribution and concentration into layers and nodules, the second phase of the cementation did not occur until the later stage of the burial during favourable thermal convection. The chlorite cement is attached to the quartz grains in the open marine facies, and post-dates the calcite cement, the iron-ooids and the siderite in the examined facies. Chlorite cements are usually formed early during diagenesis and are largely confined to marginal marine beds (cf. Humphreys et al. 1989) as the open marine sandstone. The development of secondary porosity has probably appeared during two stages, where the latter has been the dominant. The secondary pores in the massive sandstone consist partly to almost of bitumen, hence are the introduction of oil and bitumen the last diagenetic process in the paragenetic sequence.

Clay matrix

The mineralogy of the detrital clay (kaolinite and illite) in the bioturbated and heterolithic sandstones reflects the source-area geology, climate, transport processes and weathering processes. The presence of detrital matrix in the sandstone can originate due to mass flow reworking (with floating larger grains), or due to mud matrix introduction by bioturbation. In case of the investigated samples of burrowed matrix, the bulk of the sand will be grain supported, with partly or completely filled pores, whereas only within the burrows a matrix-supported framework with floating grains may occur.

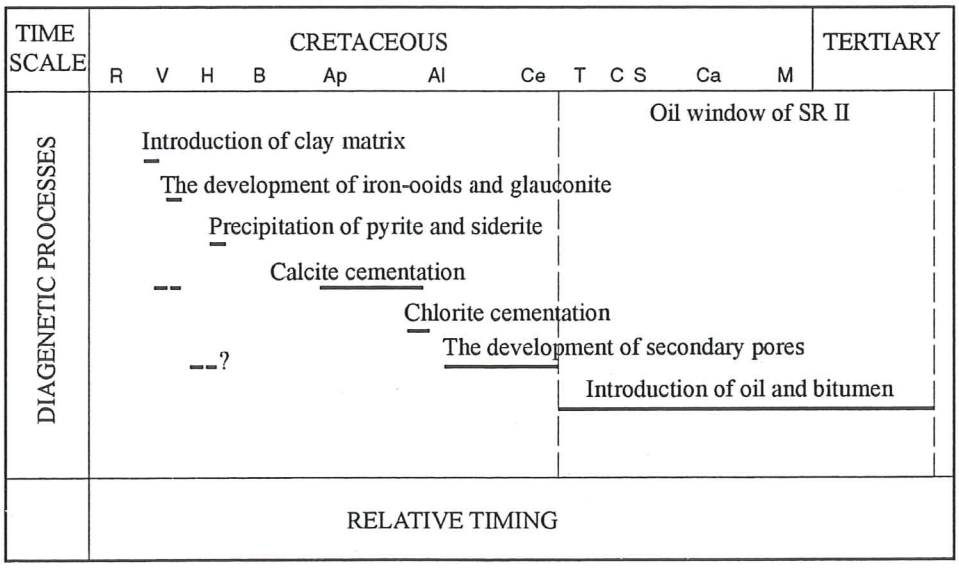

Fig. 20. Reservoir quality development in the Bentheim Sandstone from the Schoonebeek field as determined from textural relationship. (R=Ryazanian, V=Valanginian, H=Hauterivian, B=Barremian, Ap=Aptian, Al=Albian, Ce=Cenomanian, T=Turonian, C=Coniacian, S=Santonian, Ca=Campanian and M=Maastrichtian).

Matrix can also be introduced into the sediments by infiltration (above groundwater level), where the detrital matrix only partly fills the pores with lined clay laminae or cutans (cf. Molenaar 2002). The matrix in the bioturbated sandstone reflects the burrowing activity in the sediment. The matrix in the sandier parts of the heterolithic sandstone indicates that the matrix is a combined effect of disturbed clay laminae and lower intensity of bioturbation. The open marine facies is more complex and the matrix can primarily be related to intense marine biological reworking processes of the sediment. Clay matrix is harmful for reservoir quality (Fig. 21).

Hartmann (2000) suggested that detrital clay might also contribute with ions. This contribution is important to authigenesis and cementation processes during later burial diagenesis.

Calcite and chlorite cement

Calcite cement is present in all cores, and has been identified by means of XRD, PPL and SEM. Calcite is one of the most common cements types in sandstone in general (Tucker 1991). Calcite cements are common in grain-supported sandstones (85-90% in entire carbonate cemented layers and 30-35%) in the nodules. According to Tucker (1991) early precipitation of calcite may inhibit later development of quartz overgrowths and feldspar alteration to clay minerals. However, it also results in the immediate loss of porosity and permeability and reduces the reservoir quality. The quartz grains in sandstones cemented by calcite commonly have corroded

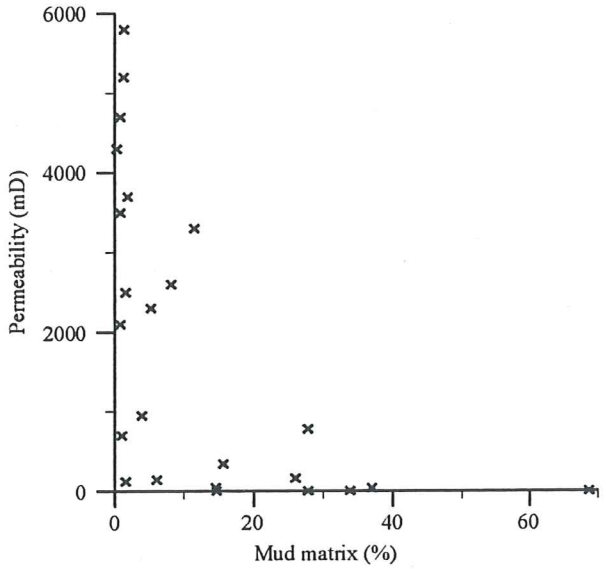

Fig. 21. Permeability plotted against mud matrix. Samples with high permeability show low matrix contents. However, in some samples the permeability is more connected other diagenetic features such as precipitation of pyrite and siderite, development of glauconite grains and iron ooids, precipitation of calcite and chlorite cement, and development of secondary pores and the introduction of oil and bitumen. The microporosity is the effect of illite being present in the detrital matrix (5-15% of the total porosity). According to Hurst & Nadeau (1996) illite commonly has microporosity of approximately 90%. Whereas in the open marine sandstone the high microporosity is related to matrix of mud, silt and very fine quartz (20-45% of the total porosity).

margins, as observed in the massive sandstone. The lithification by marine carbonate cementation of sands enriched in detrital carbonates and bioclasts can be rapid and may occur in highstand and lowstand system tracts (Friedman 1998). Early calcite lithification often leads to the stabilisation of the grain framework, which may prevent porosity destruction by compaction during subsequent burial (Worden 1998). The appearance of carbonate-cemented layers and nodules can, according to Walderhaug & Bjørkum (1998) be explained by ions derived from the dissolution of local biogenic carbonate grains and diffusional redistribution and preferential precipitation in certain locus during burial and favourable thermal convection. Another potential source of calcium carbonate is supersaturated seawater that acts as an external source providing the sand with cations (Mg^{+} and Ca^{+}) and anions (HCO_3^{-}) to develop calcite cement during early diagenesis at or near the sea floor. These (HCO_3) ions can be derived from dissolution of detrital carbonate or organic reactions of kerogen. In the Schoonebeek field, cementation both from external and internal sources is controlled by the initial concentration of carbonate grains, permeability and flow or seawater during periods of low net sedimentation rates and the carbonate-cemented nodules that are usually bounded by impermeable layer (cf. Molenaar 1998). The bioclasts both in the carbonate-cemented layers and in nodules often show a neomorphism, which suggests a change in the diagenetic environment.

Chlorite cement is only present in the open marine sandstone, where the cement is attached to the quartz grains. Chlorite cements are usually formed early during diagenesis and are generally confined to marginal marine beds (cf. Humphreys et al. 1989), as seen in the investigated open marine sandstone category of this study.

Iron minerals in sandstones

The precipitation of pyrite, siderite, glauconite and iron-ooids probably reflect the chemical conditions in the depositional environment as these minerals commonly form in the early diagenetic stage, shortly after deposition and within the sediment. Glauconite minerals contain both Fe^{2+} and Fe^{3+} and thus reflect sub-oxic conditions. Pyrite, and siderite were formed in an anoxic environment, where pyrite develops from reduced iron and hydrogen sulphide and is a common authigenic precipitate in organic-rich estuarine and tidal-flat sediments (Tucker 1991). Siderite occurs as early cement in open marine sandstones and precipitates in marine environment during reducing conditions after the exhaustion of sulphur (pyrite formation) (methanogenic zone) (Stonecipher 1999). The most common place for siderite nodules to form is in coal basins far from marine settings (Ahlberg personal comments 2002). Authigenic glauconite normally develops on outer margins of continental shelves in areas of low sediment input because its precursors need to remain at or near the sediment-water surface for long periods of time (K^{+} accumulates from sea water) where they can be repeatedly exhumed and shallow buried (Stonecipher 1999). Iron-ooids develop in shallow-ma-

rine settings and are likely to form from the precipitation of iron, aluminium and silica derived from fluids in the sediment (Heikoop et al. 1996). Sturesson et al. (2000) stated that the enrichment in these elements are in asso-caition with active volcanism, which indicates that volcanic matter could be the source of cations for many of acient iron-ooids.

Leaching and secondary porosity

In the Bentheim Sandstone, calcite and feldspars have been dissolved. This have occurred in the Schoonebeek cores as leaching and the secondary pores possible developed during two phases, by meteoric flushing during early burial and by aggressive pore fluids in subsurface environment due to maturation of kerogen. The latter mechanism probably had the dominant effect, because of the high net sedimentation, and the high subsidence rate of the Bentheim Sandstone

The presence of secondary porosity is widespread within the three Schoonebeek cores. Giles (1987) concludes that secondary porosity is likely to form due to the decomposition of diagenetically unstable minerals. Schmidt & McDonald (1979) instead stated that the classification of secondary pores must be based upon their origin and pore texture. Intergranular and moldic oversized pores of the Schoonebeek cores reflect the dissolution pattern and the fluid that causes the leaching of detrital particles such as feldspar, fossil debris and intergranular cements. Early diagenetic carbonate dissolution generally creates most of the secondary porosity (Giles & de Boer 1989). The leaching and secondary porosity improves the reservoir quality significantly due to the enhancement of the petrophysical properties.

Several mechanisms have been proposed control the flow and composition of pore fluids. These resulted in dissolved detrital minerals and the development of secondary pores. Giles & Marshall (1986) listed the most popular of these mechanisms:

- Meteoric flushing (Bjørlykke 1984);
- Mixing corrosion (Bögli 1964; Plummer 1975);
- Acid fluids generated from CO_2 produced during thermal maturation of organic matter (Schmidt & McDonald 1979);
- Carboxylic acids generated during the thermal maturation of organic matter (Surdam et al. 1984);

Reactions generated by clay mineral transformations in shales (Bjørlykke 1984).

The meteoric flushing and the aggressive pore fluids (due to maturation of kerogen) have developed the leaching and secondary porosity. This can be related to the unaffected K-feldspar in the detrital clay in the bioturbated sandstone, and the abundant of secondary pores in the hydrocarbon charged sediments. Hence, these mechanisms have affected the Bentheim Sandstone during different stages of burial. Because of the apparent difficulty to move large quantities of solutes through sandstones during deep burial, Bjørlykke (1984) suggested that the majority of secondary porosity form during early burial under the influence of meteoric water flushing. The Bentheim Sandstone has probably been sparsely affected by the meteoric fluid due to the rapid subsidence of the succession in this part of the LSB, because of the relative short time the pore fluids had the opportunity to pass through the strata (Wonham et al. 1997).

Scherer (1987) stated that leaching in subsurface environments could develop significant quantities of secondary porosity. A hypothesis for the generation of a dissolving active fluid in the subsurface is that of CO_2 produced during the thermal maturation of hydrocarbon source rocks and coals, where the CO_2 creates an aggressive pore fluid of HCO_3^- and H^+ (in equilibrium) (Giles & Marshall 1986). In fact, several organic compounds may affect the environment, lower the pH, and change the Eh thus causing leaching conditions. Surdam et al. (1993) observed that redox reactions associated with an influx of hydrocarbons into the sandstone significantly could enhance the secondary porosity and dissolution of carbonate fragments. In the massive sandstone of core Sch-590, bitumen is present in the secondary pores. Hydrocarbon originated from the Berriasian age is emplaced in the overlaying Bentheim succession has the short distance between the source rock and the reservoir rock would significant set off this effect. The dissolution and alteration of chemically unstable minerals such as K-feldspar, calcite and, detrital clay minerals may enhance the intergranular and moldic porosity in the Bentheim Sandstone. Hartmann et al. (2000) stated that the dissolution provides a variety of ions that is closely connected the precipitation of most late diagenesis phases such as authigenic quartz, feldspar, calcite and kaolinite in the sediment, which consequently have a decreasing effect of the porosity and permeability. The amount of authigenic clay is low in the Schoonebeek cores, where almost all clay in the sandstone is detrital. To the contrary, in the Bentheim Sandstone in the outcrop at Gildehaus, authigenic kaolinite-dickite fills part of the secondary pores.

Discussion

The original clastic mineralogy and the good sorting of the Bentheim Sandstone initially promoted very good reservoir qualities, which had a high potential to survive even during deep burial. Because of the quartz rich composition and the mechanical and chemical stability of the quartz grains, the initial porosity and permeability survived. It is obvious from the porosity data that mechanical compaction did not occur. Nagtegaal (1977) stated that coarse-grained, well-sorted pure quartz arenites have optimal potential of preserving high depositional porosity and permeability during burial diagenesis, such as the Bentheim Sandstone (in particular the massive sandstone).

The lack of quartz cementation in the investigated subcrop sandstone facies makes the reservoir dependent on the primary qualities of the sandstone and the net sedimentation rate. Thus, the combined effects of compaction, the content of detrital clay and the secondary porosity development cause variation in total porosity. The massive sandstone facies has the highest net sedi-

mentation rate and the highest value of porosity and permeability (this study and Wonham et al. 1997).

The massive sand is the category with the highest porosity and permeability. This can be related to its low concentration of detrital clay and the abundant secondary porosity. The secondary pores are often oversized in appearance and could not be correlated with the K-feldspar grain size. Therefore, the oversized pores probably represent dissolved carbonate fragments. The bioturbated and the heterolithic sandstone show a range in porosity and permeability, which reflects the presence of detrital clay. Despite a high concentration of detrital clay the measured porosity is still high in the bioturbated and the heterolithic sand facies. This probably indicates microporosity within the detrital clay. The permeability is affected by the amount of detrital clay, which results in a decreasing reservoir quality with an increase in clay concentration. The heterolithic silt-mud partings differ from the other examined facies in terms of permeability. This facies shows considerable permeability horizontally, and blocked vertical migration pathways (anisotropic permeability, see Ahlberg & Olsson 2001).

The open marine sandstone shows high porosities and very low permeabilities in conjunction with abundant detrital clay content indicated by petrophysical measurement. The open marine sandstone is heterogeneous in mineralogical composition and in the lowermost parts of the facies the matrix is mainly a mixture of mud, silt and very fine quartz. Chlorite and calcite cement is also present. In the upper parts of the open marine sandstone sequence, calcite cement dominates and only minor chlorite cement is present. The open marine sandstone was probably developed by different reworked sediments, which have been re-deposited, including palaeosols. Some of the iron-ooid occurrence has not as smooth outer surface as iron-ooids. The different ooid structures may be precipitated in a soil environment. Glauconite is present as grain concentrations. The high porosity values are more a result of a mix of microporosity in the clay and pores as dissolution around iron-ooids and oncoid structures. However, the microporosity contributes to the porosity but cannot be negatively related to permeability.

The absence of quartz cementation is conspicuous in all three studied cores and in all subcrop sandstone facies. The emplacement by clay minerals and bitumen of the "pure" quartz grain nucleus probably played a significant role in preserving high porosity and permeability. However, microporosity in the detrital clay and the secondary porosity also may have contributed to the high values in porosity and permeability for this burial depth. In Haltenbacken, North Sea, Ehrenberg (1990) observed that mechanical compaction has been more important than quartz cementation in reducing porosity. This can also be the case in Bentheim Sandstone, where more porosity has been lost by compaction than by the effect of diagenesis.

Fine-grained sandstones are more resistant to mechanical compaction at depths of less than 2 km, whereas in sandstones buried more than 2 km depth, chemical compaction becomes important due to intergranular pressure dissolution (Ehrenberg 1990). There is no evidence of significant pressure dissolution in the Schoonebeek cores. Moreover, intergranular porosity has not been reduced by quartz cementation. The high porosity of the massive sandstones is related to the preservation of much of the primary porosity and to the presence of secondary pores. The dissolution of some K-feldspars at great depths may have progressively changed the sandstone composition from a more arkosic arenite to the present day quartz arenite (cf. Haszeldine 2000). The development of secondary pores has probably enhanced both porosity and permeability in the massive sandstone, where the dissolution has been the result of the circulation of dissolving fluids or the generation of acids. The presence of corroded grains, carbonate cement and oversized pores indicates that aggressive fluids initiated partial or complete destruction of these materials. This dissolution and the development of secondary pores can be correlated to either meteoric flushing and to the generation of organic acids during burial with the development of hydrocarbon maturity in the Berriasian source rock. This leaching hypothesis relies on the production of CO_2 and organic acid during thermal kerogen maturation in the pore water (Giles & Marshall 1986). To support this idea a significant fluid flow must have occurred in the sediment during the time of hydrocarbon maturity and later migration of hydrocarbon into the reservoir rock (Bentheim Sandstone). The low amount of authigenic clay and the high content of dissolved K-feldspar reflect ion transport by means of pore water flux in the sediment. An 'open' system porosity enhancement like this involves removal of material from the leached deposits (Giles 1987).

General comparisons between different cores commonly show that decreasing reservoir quality reflects different degrees of diagenetic alteration rather than variations in primary sand quality (Ehrenberg 1990). This does not fit to the petrographic properties of the three studied cores. In there, the reservoir quality is due to the rapid subsidence in the Emsland area of the LSB and that porosity and permeability depends on the subsidence rate and thickness of the deposited sediment (Wonham 1997). Wonham et al. (1997) observed that in areas of high subsidence sandstones developed with less abundant mud drapes due to the higher energy of the depositional environment, with considerably porosity and permeability. This implies that the primary distribution of the sediment plays a significant role for the result in porosity and permeability. This can also be seen in the concentration of mud matrix, distribution of secondary pores derived to depositional environment (Table 5 and 6).

The trend (Fig. 16) shows that an increase in secondary pores often increases the petrophysical properties. Consequently, this leads to the assumption that detrital K-feldspar and carbonate grain content and the acid fluids that resulted in leaching and the development of secondary pores largely control the reservoir quality of the Bentheim sandstone in the Schoonebeek field. The massive sandstone proved to have the highest occurrence of secondary pores and the best petrophysical properties.

The appearance of secondary porosity therefore explains the excellent reservoir quality of the massive sandstone. The microporosity contributes to the porosity but cannot be correlated to the permeability.

The kaolinite content and the possible later emplacement of authigenic illite are related to the depositional features and the clay that is present in the sandstone is derived to the content of detrital clay. The AAS shows that K and Al correlates and can be completely assigned to detrital clays. If the samples Pm 112 and Pm 216 are disregarded Mg and Al correlates, suggesting that Mg is part of clay mineral. There is a very low amount of authigenic clay in the oil-saturated facies and this has also contributed to the preservation of the porosity and permeability in Bentheim Sandstone during diagenesis. Potentially it has also inhibited the alteration of kaolinite to illite (or, the content of detrital illite was too low).

The LECO analysis showed that bitumen is present in the massive, heterolithic and bioturbated sandstone and the PPL confirms that bitumen occurs in secondary pores. Due to the closeness of the source rock and the seals of the reservoir (see Fig. 3), the oil emplacement has contributed to favourable processes such as enhanced porosity (development of secondary porosity). According to Giles et al. (2000) the process of blocking "pure" nucleus inhibits the effect of quartz cementation and authigenic clay development. However, where the dissolution is accompanied by a precipitation of an almost identical volume of authigenic minerals, secondary porosity may not cause a real increase in porosity, rather a redistribution of porosity (a redistribution of mass and pores in the sediment; see Giles 1987). The favourable oil emplacement has showed that oil charging may preserve porosity in oil fields during burial (Haszeldine et al. 2001). Shebl et al. (1996) show that CO_2 and organic acids from hydrocarbon source rocks are capable of destabilising carbonate cements and carbonate fragments. The dissolution of these unstable grains and cements increases porosity. The presence of the carbonate-cemented nodules and layers can be related to the reaction of acetic acid and carbonate minerals that enhances porosity and results in the release of Ca^{2+} (Surdam et al. 1993). In this instance the redox reactions may explain not only the zones of porosity enhancement associated with hydrocarbon accumulation, but also those of the observed carbonate-cemented nodules and layers (Surdam et al. 1993).

The presented study shows that the lowest amount of detrital clay occurs in the massive sandstone. Carbonate-cemented beds and the highest content of secondary pores are also present in this category. This, in turn, has created the best reservoir qualities of the compared sandstones in the Schoonebeek cores.

Comparison between Bentheim Sandstone subcrop (Schoonebeek) and outcrop samples (Gildehaus) in petrophysical properties

The subcrop and the outcrop study area are located on opposite sides of an anticline. The subcrop has been charged with hydrocarbon whereas the outcrop was not. The porosity and permeability preservation of the Bentheim Sandstone in the outcrop samples is partly due to the preservation of primary porosity by limited stabilising quartz cementation (Plate 2, Fig. 22) and by secondary moldic porosity through dissolution of feldspars. The stable grains and limited cementation supported the framework and consequently the oversized secondary pores were preserved and did not cause framework collapse by mechanical compaction in both outcrop and subcrop samples. The cementation in the outcrop is more due to quartz cement, whereas in the subcrop the cementation reflects the early precipitation of calcite cement. The quartz cement in the outcrop samples was derived from the dissolution of detrital feldspars, which released silica to the pore water (Mansurbeg 2001). Due to this, the Gildehaus petrophysical properties have been affected negatively by the quartz cementation (Mansurbeg 2001). Another possible source of silica in the Gildehaus is pressure dissolution and re-precipitation (Plate 2, Fig. 23). The subcrop samples have detrital appearances similar to those of the Gildehaus samples, but the former were affected by hydrocarbon charging, which inhibited quartz cementation and enhanced porosity. Thus, reduced intergranular porosity due to quartz cementation is an important difference between the outcrop samples from Gildehaus Quarry and the Schoonebeek cores (Plate 2, Fig. 24). They show a higher content of the petrographical properties than the outcrop samples do.

The other difference is the abundance of oversized pores due to carbonate fragment dissolution in the subcrop cores compared to the general appearance of partly to almost dissolve K-feldspars in the outcrop material.

In both outcrop and subcrop samples the original detrital feldspar content has had a profound effect on modifying the primary petrophysical properties, which has resulted in less arkosic sandstones. In the Schoonebeek cores the dissolution and development of secondary pores (both dissolved K-feldspars and carbonate fragments) potentially occurred in two phases, during shallow burial depth and during hydrocarbon maturation in the subsurface. Whereas the oversized (secondary) pores in the Gildehaus were formed due to dissolution of detrital feldspar grains at shallow burial depth. The Schoonebeek and Gildehaus material shows that potassium (dervided due to K-feldspar dissolution), and possibly calcium has been transported out of the sandstone system. The study of the Schoonebeek and Gildehaus material suggests that the diagenetic system was at least partly open during diagenesis. In Gildehaus, authigenic kaolinite affected the permeability significantly (cf. Mansurbeg 2001), whereas in Schoonebeek the low permeability in bioturbated, heterolithic and open marine sandstones reflect low-energy depositional environment and bioturbation of detrital clay.

Potential as reservoir rock

The present study of the depositional and the diagenetic properties implies that the Bentheim Sandstone of the Schoonebeek field has a good reservoir quality. However, the quality is facies dependent. The bioturbated sandstones of the Bentheim Sandstone formation are matrix

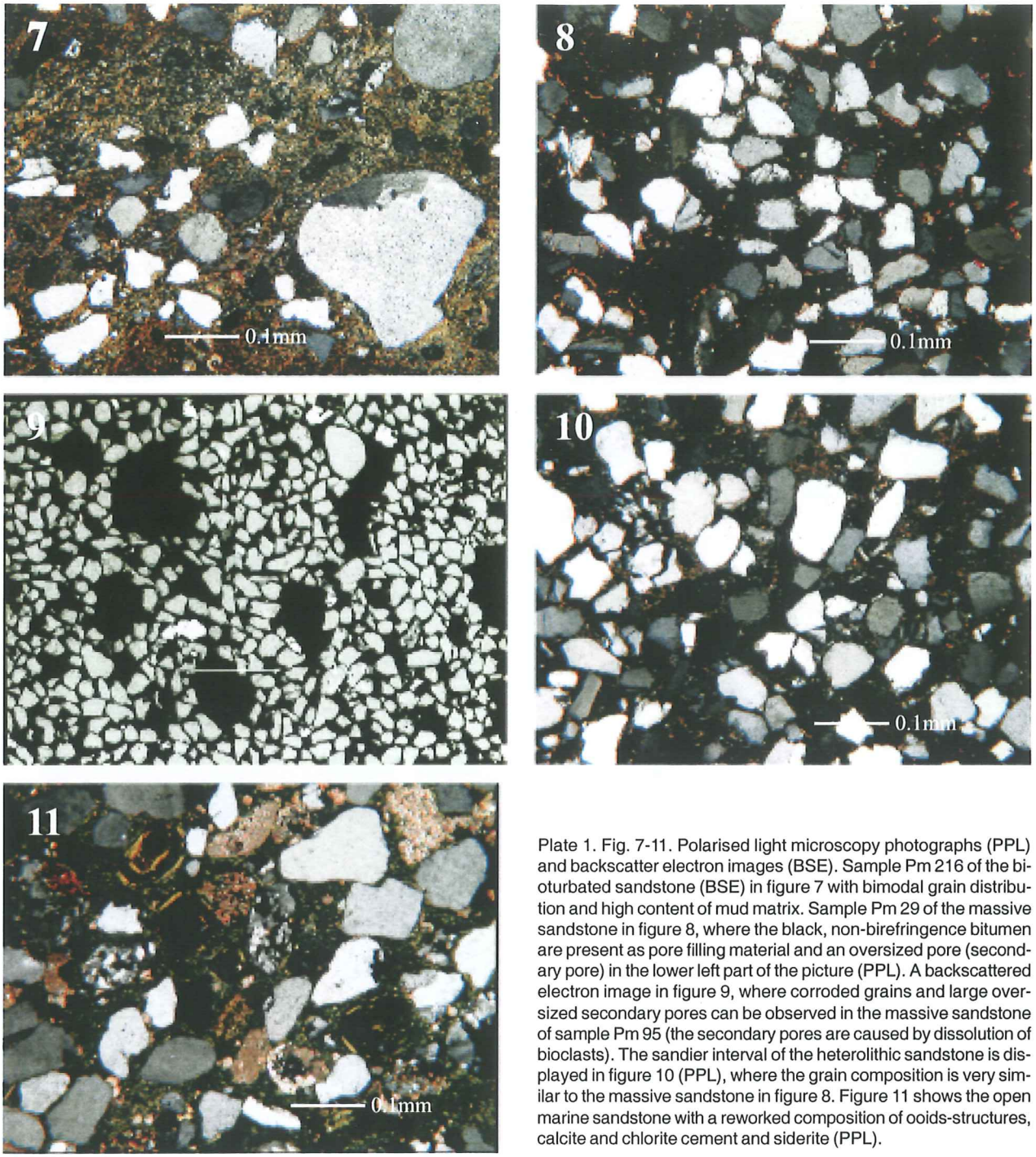

Plate 1. Fig. 7-11. Polarised light microscopy photographs (PPL) and backscatter electron images (BSE). Sample Pm 216 of the bioturbated sandstone (BSE) in figure 7 with bimodal grain distribution and high content of mud matrix. Sample Pm 29 of the massive sandstone in figure 8, where the black, non-birefringence bitumen are present as pore filling material and an oversized pore (secondary pore) in the lower left part of the picture (PPL). A backscattered electron image in figure 9, where corroded grains and large oversized secondary pores can be observed in the massive sandstone of sample Pm 95 (the secondary pores are caused by dissolution of bioclasts). The sandier interval of the heterolithic sandstone is displayed in figure 10 (PPL), where the grain composition is very similar to the massive sandstone in figure 8. Figure 11 shows the open marine sandstone with a reworked composition of ooids-structures, calcite and chlorite cement and siderite (PPL).

rich due to biogenic mixing of mud and sand laminae. The reservoir quality depends on the matrix content. Pyrite is locally pore filling and decreases the permeability. Detrital kaolinite and illite significantly affect the permeability negatively.

The massive sandstone, with the highest net sedimentation rates, has the highest porosity and permeability, due to the low concentrations of detrital clays and to the abundance of secondary pores. The secondary pores are partly of oversized appearance and match the size and shape of dissolved carbonate fragments. The massive sandstone shows the best reservoir qualities in the studied Schoonebeek cores.

The heterolithic sandstone shows a spread in porosity and permeability values, which reflects the variable effect of detrital clay (illite and kaolinite). This category differs from the other facies in showing a directional trend of permeability. The clay laminae block vertical permeability whereas the horizontal permeability is higher (permeability anisotropy). The reservoir quality is good in the well-sorted sand intervals.

The open marine sandstone has a high porosity and a very low permeability, as a result of the high content of detrital clay. The category was affected by reworking of the sediment and various materials occur from different diagenetic stages. The high porosity is a result of micro-

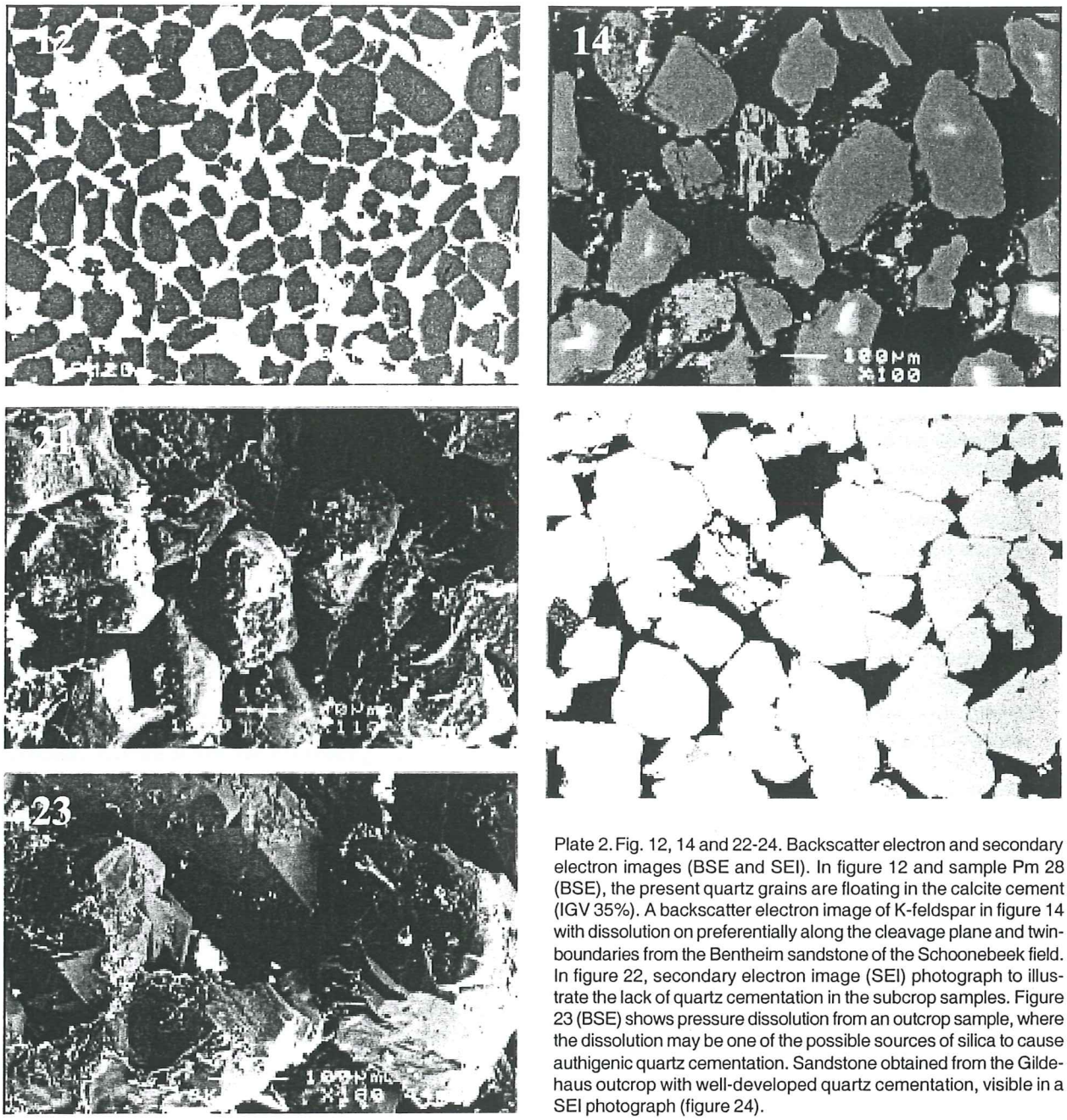

Plate 2. Fig. 12, 14 and 22-24. Backscatter electron and secondary electron images (BSE and SEI). In figure 12 and sample Pm 28 (BSE), the present quartz grains are floating in the calcite cement (IGV 35%). A backscatter electron image of K-feldspar in figure 14 with dissolution on preferentially along the cleavage plane and twin-boundaries from the Bentheim sandstone of the Schoonebeek field. In figure 22, secondary electron image (SEI) photograph to illustrate the lack of quartz cementation in the subcrop samples. Figure 23 (BSE) shows pressure dissolution from an outcrop sample, where the dissolution may be one of the possible sources of silica to cause authigenic quartz cementation. Sandstone obtained from the Gildehaus outcrop with well-developed quartz cementation, visible in a SEI photograph (figure 24).

porosity in the clay matrix and partial dissolution of iron-ooids. The permeability is negligible and insufficient for a reservoir point of view.

Conclusions

The aim for this work was a re-evaluation of the petrographic and sedimentological parameters concerning the Schoonebeek hydrocarbon reservoir to aid the assessment of its future potential.

The porosity of the Bentheim Sandstone in the Schoonebeek field consists of primary pores, related to the depositional texture, and of secondary pores developed during burial diagenesis. The heterogeneity in the reservoir is mainly related to distribution of depositional facies.

During kerogen maturation of the Berriasian paper-shales, aggressive pore fluids developed that enhanced the porosity in the Schoonebeek cores. The subsequent charging of hydrocarbons into the Bentheim Sandstone blocked the "pure" quartz nuclei, which inhibited quartz cementation and authigenic clay development in the sandstones. Where hydrocarbons were absent, both of these processes took place in the Bentheim Sandstone as seen at the Bentheim and Gildehaus outcrops. The low amount of authigenic clay and the high content of dissolved K-feldspar and carbonate fragments suggest that ion transport occurred in the sediment, in a semi-closed or open system.

Other diagenetic processes such as mechanical compaction only had minor effect on porosity due to the mechanical stable mineralogical composition of the quartz-

rich sandstones. During early burial diagenesis, carbonate cement precipitation resulted in cemented layers and isolated nodules. The early diagenetic calcite cement prevented compaction and framework collapse and preserved much of the primary porosity and prevented dissolution of detrital grains.

The carbonate-cemented layers represent stratabound impermeable layers, developed by ion redistribution of local biogenic carbonate. Corroded grains and calcite cement in the Bentheim Sandstone suggest that the carbonate-cemented horizons were more extensive prior the maturation of the hydrocarbons.

Acknowledgements

I want to thank my supervisors Dr. Nicolaas Molenaar at the Technical University of Denmark (DTU) and Dr. Anders Ahlberg at Lund University (LU) for their generous help. Dr. Nicolaas Molenaar is also thanked for all useful comments on earlier versions of the manuscript. Furthermore, I like to thank Sinh Niguyen, Zoltan Solyom and Takeshi Miyazu for the help with conducting the analyses. Kirsten Jensen is thanked for the assistance with the preparation of thin section and "stubs". So are Willem Schuurman and the technicians in the core storage at NAM for their generous hospitality during my visit in Assen, Henrik Jonsson for his support during the writing process, Annika Jilkén for everything and all my friends for their support. Without the help of the NAM, kindly providing the petrophysical data and the sample material, this study would not have been possible.

References

Aagaard, P., Bjørlykke, K., Egeberg, P.K., Saigal, G.C., & Morad, S., 1990: Diagenetic albitization of detrital K-feldspar in Jurassic, Lower cretaceous and Tertiary clastic reservoir rocks from offshore Norway, II, Formation water chemistry and kinetic considerations. *Journal of Sedimentary Research 60*, 575-581.

Ahlberg, A., & Olsson I., 2001: Petroleum assessment of the Mesozoic succession in the Höllviken Graben and the Skurup Platform, southern Sweden. *GFF 123*, 85-95.

Betz, D., Fuhrer, F., Greiner, G., & Plein, E., 1987: Evolution of the Lower Saxony Basin. *Tectonophysics 137*, 127-170.

Björlykke, K., 1984: Formation of secondary porosity: How important is it? *AAPG Memoir 37*, 277-286.

Björlykke, K., & Egeberg, K.P., 1993: Quartz cementation in sedimentary basins. *AAPG Bulletin 77*, 1538-1548.

Budd, D., Hammes, U., & Ward, W.B., 2000: Cathodoluminescence in calcite cements, new evidence on Pb and Zn sensitising, Mn activation, & Fe quenching at low trace-element concentrations. *Journal of Sedimentary Research 70*, 217-226.

Bögli, A., 1964: Mischungskorrosion, ein Beitrag zum Verkarstungsproblem. *Erkunde 18*, 83-92.

Ehrenberg, N.S., 1990: Relationship between diagenesis and reservoir quality in sandstones of the Garn formation, Haltenbanken, Mid- Norwegian continental shelf. *AAPG Bulletin 74*, 1538-1558.

Friedman, G.M., 1998: Rapidity of marine carbonate cementation- implications for carbonate diagenesis and sequence stratigraphy: perspective. *Sedimentary Geology 119*, 1-4.

Füchtbauer, H., 1955: Zur Petrographie des Bentheimer Sandsteins in Emsland: *Erdöl und Kohle 8*, 616-617.

Füchtbauer, H., 1963: Paleogeograph and reservoir properties of the Lower Cretaceous „Bentheim Sandstone". In: *Excursion Guide Book 1*, 6th World Petroleum Congress (Hannover), 42-43.

Giles, M.R., & Marshall, J. D., 1986: Constraints on the development of secondary porosity in the subsurface: Re-evaluation of processes. *Marine and Petroleum Geology 3*, 243-254.

Giles, M.R., 1987: Mass transfer and problems of secondary porosity creation in deeply buried hydrocarbon reservoirs. *Marine and Petroleum Geology 4*, 188-204.

Giles, M.R., Indrelid, G.V., Beynon and Amthor, J., 2000: The origin of large-scale quartz cementation evidence from large data sets and coupled heat-fluid mass transport modelling. In: *Quartz cementation in sandstones.* R.H Worden & S. Morad (eds.): IAS Special Publication 29, 1-20.

Gradstein, F.M, Agterberg, F.P., Ogg, J.G., Hardenbol, J., van Veen, P., Thierry, J., & Huang Z., 1994: A Mesozoic time scale. *Journal of Geophysical Research 99*, 24051-24074.

Grote-Sedlácek, R., 1984: Untersuchung der Vertonung im Bentheimer Sandstein des Erdölfeldes Rühlermoor mit Hilfe von Bohrlochmessungen und Kerninformationen. Ph.D. Dissertation aus Ohlendorf/Kreis Harburg.

Hartmann, B.K., Juhász-Bodnár, K., Ramseyer, K., & Matter, A., 2000: Polyphased quartz cementation and its sources: a case study from the Upper Palaeozoic Haushi Group sandstones, Sultanate of Oman. In: *Quartz cementation in sandstones.* R.H Worden & S. Morad (eds.): IAS Special Publication 29, 253-270.

Haszeldine, S.R., Macaulay, C.I., Marchand, A., Wilkinson, M., Graham, C.M., Cavanagh, A., Fallick, A.E., & Couples, D.G., 2000: Sandstone cementation and fluids in hydrocarbon basins.?????????

Haszeldine, S.R., Marchand, A., Smalley, P.C., Macaulay, C.I., & Fallick, A.E., 2001: Evidence for reduced quartz cementation rates in oil-filled sandstones. *Geology 29*, 915-918.

Heikoop, J.M., Tsujita, C.J., Risk, M.J., Tomascik, T., & Mah, A.J., 1996: Modern iron ooids from shallow-marine volcanic setting: Mahengtang, Indonesia. *Geology 24*, 759-762.

Hinze, C., 1988: Geologische Karte von Niedersachsen 1:25000. *Erläuterungen zum Blatt 3608 (Bad Bentheim)*, 120 pp. (Niedersächsisches Landesamt für Bodenforschung, Hannover).

Humphreys, B., Smith, S.A., & Strong, G.E., 1989: Authigenic chlorite in late Triassic sandstones from the Central Graben, North Sea. *Clay Minerals 24 (2)*, 427-444.

Hurst, A., & Nadeau, P.H., 1996: Clay microporosity in reservoir sandstones: an application of quantitative electron microscopy in petrophysic evaluation. *International Journal of Rock Mechanics and Mining Sciences and Geomechanics Abstracts 33 (1)*, 18A.

Kemper, E., 1968: Einige Bemerkungen über die Sedimentationsverhältnisse und die fossilen Lebensspuren des Bentheimer Sandsteins (Valanginium). *Geologisches Jahrbuch. 86*, 49-106.

Kemper, E., 1976: Geologischer Führer durch die Grafschaft Bentheim und die angrenzenden Gebiete mit einem Briss der emländischen Unterkreide. In: *Das Bentheimer Land* (eds Heimatverein der Grafschaft Bentheim) 64, 206 pp. (Verlag Heimatverein der Grafschaft Bentheim e.V., Nordhorn-Bentheim).

Kockel, F., Wehner, H., & Gerling, P., 1994: Petroleum systems of the Lower Saxony Basin, Germany. *AAPG Memoir 60*, 573-586.

Kortmann, H., 1983: Sedimentologische Untersuchungen über den Bentheimer Sandstein (Valangin). (Sedimentological analysis of the Bentheim Sandstone (Valanginian) in the area of the Bad Bentheim). Diplomarbeit, Geologischen Insititut der Universität zu Köln.

Mansurbeg, H., 2001: Modelling of reservoir quality in quartz-rich sandstone of the Lower Cretaceous Bentheim Sandstone, Lower Saxony Basin, NW-Germany.

Miller, J., 1988: Cathodoluminescence microscopy. *Techniques in Sedimentology*, 86-107. M.E. Tucker, (ed). Blackwell Science publications, Oxford.

Molenaar, N., 1998: Origin of low-permeability calcite-cemented lenses in shallow marine sandstones and $CaCO_3$ cementation mechanisms: an example from the Lower Jurassic Luxemburg Sandstone, Luxemburg. *Carbonate Cementation in Sandstones.* S. Morad (eds.). IAS Special publication 26, 193-211.

Morad, S., 1998: Carbonate cementation in sandstones: distribution patterns and geochemical evolution. *Carbonate Cementation in Sandstones.* S. Morad (eds.). IAS Special publication 26, 1-26.

Mutterlose, J., 1995: Die Unterkreide-Aufschlüsse des Osning-Sandsteins (NW-Deutschland)-Ihre Fauna und Lithofazies. *Geologie und Paläontologie in Westfalen 36*, 1-85.

Mutterlose, J., & Bornemann, A., 2000: Distribution and facies of Lower Cretaceous sediments in northern Germany: a review. *Cretaceous Research 21*, 733-759.

Nagtegaal, P.J.C., 1978: Sandstone-framework instability as a function of burial diagenesis. *Journal of geological Society of London, 135*, 101-105.

Parnell, J., Ruffel, A.H., Monson, B., & Mutterlose, J., 1996: Petrography and origin of deposits at the Bentheim bitumen mine, north western Germany. *Mineralium Deposita 31*, 104-112.

Owen, M.R., 1991: Applications of Cathodoluminescence to sandstone provenance. *Luminescence microscopy.* C.E:, Baker & O.C., Kopp (eds.). SEPM short course 25, 67-75.

Pettijohn, F.J., Potter, P.E., & Siever, R., 1972: *Sand and sandstones*. Springer Verlag, Berlin-Heidelberg. 618pp.

Plummer, L.N. 1975: Mixing of sea water with calcium carbonate ground water. *Memoir of the Geological Society of America. 142*, Quantitative studies in the geological sciences, 19-236.

Reading, H.G., & Levell, B.K, 1996: Controls on the sedimentary rock record. *Sedimentary Environments (Processes, Facies and Stratigraphy).* H.G. Reading (ed). Blackwell Science publications, Oxford 688pp.

Ryan, J.M., Zachry, D.L., 1997: Diagenetic controls on porosity preservation in Morrowan reservoir units, Arkoma Basin, Arkansas. *Geological Society of America 29 (6)*, 464.

Scherer, M., 1987: Parameters influencing porosity in sandstones: A model for sandstone porosity prediction. *AAPG Bulletin 71*, 485-491.

Schimdt, V., & Mcdonald, D.A., 1979: Texture and recognition of secondary porosity in sandstones. *SEPM Special Publication 26*, 209-225.

Selley, R.C., 1985: *Elements of Petroleum Geology*. W.H. Freeman and Company, New York 449pp.

Shebl, M.A., & Surdam R.C., 1996: Redox reactions in hydrocarbon clastic reservoirs: Experimental validation of this mechanism for porosity enhancement. *Chemical Geology 132*, 103-117.

Stadtler, A., 1998: *Der Bentheimer Sandstein (Valangin, NW-Deutschland).* Bochumer Geologische und Geotechnische Arbeiten 49, 123pp.

Stonecipher, S.A., 1999: Genetic characteristics of glauconite and siderite: Implications for the origin of ambiguous isolated marine sandbodies. SEPM Special publication 64, 191-204.

Strauss, C., Elstner, F., Jan du Chéne, R., Mutterloose, J., Reiser, H. and Brandt, K.-H. 1993: New micropaleontological and palynological evidence on the stratigraphic position of the "german Wealde" in NW-Germany. *Zittelina 20*, 389-401.

Sturesson, U., Heikoop, J.M., & Risk, M.J., 2000: Modern and Palaeozoic iron ooids-a similar origin. *Sedimentary Geology 136*, 137-146.

Surdam, R.C., Boese, S.W., & Crossey, L.J., 1984: The chemistry of secondary porosity. In: Clastic Diagenesis (Ed. by R.C. Surdam and D.A. McDonald). *AAPG Memoir 37*, 127-149.

Surdam, R.C. Jiao, Z.S., & MacGowan, D B., 1993: Redox reactions involving hydrocarbons and mineral oxidants: A mechanism for significant porosity enhancement in sandstones. *AAPG Bulletin 77*, 1509-1518.

Trewin, N.H., 1988: The SEM in Sedimentology. *Techniques in sedimentology.* M.E. Tucker (ed.). Blackwell Science publications, Oxford, 86-107.

Tucker, M.E., 1991. *Sedimentary Petrology*. Blackwell Science publications, Oxford 260pp.

Walderhaug, O., & Bjørkum, P.A., 1998: Calcite cement in shallow marine sandstones: growth mechanisms and geometry. *Carbonate Cementation in Sandstones.* S. Morad (eds.). IAS Special publication 26, 179-192.

Wiesner, M.G., 1983: Lithologische und Geochemische Faziesuntersuchungen an Bituminösen Sedimenten des Berrias im Raum Bentheim-salzbergen, Emsland: Ph.D. disserertion, University of Hamburg, Germany.

Wonham, J.P., Johnson, H.O., Mutterlose, J., Stadler, A., & Ruffel, A., 1997: Characterisation of a shallow marine sandstone reservoir in a syn-rift setting: The Bentheim sandstone formation of the Ruhlermoor field, Lower Saxony basin, NW Germany. *GCS-SEPM foundation 18th annual research conference shallow marine and non-marine reservoirs (Texas), December 7-10*, 427-448. Keith W. Shanley & Bob F. Perkins (eds.).

Worden, R.H. and Morad, S., 2000: Quartz cementation in oil field sandstone: a review of the key controversies. *Quartz cementation in sandstones.* R.H Worden & S. Morad (eds.). IAS Special Publication 29, 1-20.

Tidigare skrifter i serien "Examensarbeten i Geologi vid Lunds Universitet":

84. Ahlgren, Charlotte, 1997: Late Ordovician communities from North America.
85. Strömberg, Caroline, 1997: The conodont genus *Ctenognathodus* in the Silurian of Gotland, Sweden.
86. Borgenlöv, Camilla, 1997: Vätskeinklusioner som ledtrådar till bildningsmiljön för Bölets manganmalm, Västergötland, södra Sverige.
87. Mårtensson, Thomas, 1997: En petrografisk och geokemisk undersökning av inneslutningar i Nordingrågraniten.
88. Gunnemyr, Lisa, 1997: Spårämnesförsök i konstgjort infiltrerat vatten - en geologisk och hydrogeologisk studie av Strömsholmsåsen, Hallstahammar, Västmanland.
89. Antonsson, Christina, 1997: Inventering, hydrologisk klassificering samt bedömning av hydrogeologisk påverkan av våtmarksområden i samband med järnvägstunnelbyggnation genom Hallandsåsen, NV Skåne.
90. Nordborg, Fredrik, 1997: Granens mark-påverkan - en studie av markkemi, jordmånsbildning och lermineralogi i gran- och lövskogsbestånd i södra Småland.
91. Dobos, Felicia, 1997: Pollen-stratigraphic position of the last Baltic Ice Lake drainage.
92. Nilsson, Johan, 1997: The Brennvinsfjorden Group of southern Botniahalvøya, Nordaust-landet, Svalbard - structure, stratigraphy and depositional environment.
93. Tagesson, Esbjörn, 1998: Hydrogeologisk studie av grundvattnets kloridhalter på östra Listerlandet, Blekinge.
94. Eriksson, Saskia, 1998: Morängenetiska undersökningar i klintar vid Greifswalder Boddens södra kust, NÖ Tyskland.
95. Lindgren, Johan, 1998: Early Campanian mosasaurs (Reptilia; Mosasauridae) from the Kristianstad Basin, southern Sweden.
96. Ahnesjö, Jonas, B., 1998: Lower Ordovician conodonts from Köpings klint, central Öland, and the feeding apparatuses of *Oistodus lanceolatus* Pander and *Acodus deltatus* Lindström.
97. Rehnström, Emma, 1998: Tectonic stratigraphy and structural geology of the Ålkatj-Tielma massif, northern Swedish Caledonides.
98. Modin, Anna-Karin, 1998: Distributionen av kadmium i moränmark kring St. Olof, SÖ Skåne.
99. Stockfors, Martin, 1998: High-resolution methods for study of carbonate rock: a tool for correlating the sedimentary record.
100. Zillén, Lovisa, 1998: Late Holocene dune activity at Sandhammaren, southern Sweden -chronology and the role of climate, vegetation, and human impact.
101. Bernhard, Maria, 1998: En paleoekologisk -paleohydrologisk undersökning av våtmarks-komplexet Rolands hav, Blekinge.
102. Carlemalm,Gunnar, 1999: En glacialgeologisk studie av morän och moränfyllda sprickor i underliggande sandursediment, Örsjö, Skåne.
103. Blomstrand, Malou, 1999: 1992-1998 Seismicity and Deformation at Mt. Eyjafjalla-jökull volcano,South Iceland.
104. Dahlqvist, Peter, 1999: A Lower Silurian (Llandoverian) halysitid fauna from the Berge Limestone Formation, Norderön, Jämtland, central Sweden.
105. Svensson, Magnus A., 1999: Phosphatized echinoderm remains from upper Lower Ordovician strata of northern Öland, Sweden - preservation, taxonomy and evolution.
106. Bengtsson, Anders, 1999: Trilobites and bradoriid arthropods from the Middle and Upper Cambrian at Gudhem in Västergötland, Sweden.
107. Persson, Christian, 1999: Silurian graptolites from Bohemia, Czech Republic.
108. Jacobson, Mattias, 1999: Five new cephalopod species from the Silurian of Gotland.
109. Augustsson, Carita, 1999: Lapillituff som bevis för underjurassisk vulkanism av strombolikaraktär i Skåne.
110. Jensen, Sigfinn J., 1999: En silurisk transgressiv karbonatlagerföljd vid S:t Olofsholms stenbrott, Gotland.
111. Lund, Mats G., 1999: En strukturgeologisk modell för berggrunden i Sarvesvagge - Luottalako-området, Sareks Nationalpark, Lappland.
112. Magnusson, Jakob, 1999: Exploration of sub-marine fans along the Coffee Soil Fault in the Danish Central Graben.
113. Wickström, Jenny, 1999: Conodont bio-stratigraphy in Volkhovian sediments from the Mäekalda section, north-central Estonia.
114. Sjögren, Per, 1999: Utmarkens vegetations-utveckling vid Ire i Blekinge, från forntid till nutid - en pollenanalytisk studie.
115. Sälgeback, Jenny, 1999: Trace fossils from the Permian of western Dronning Maud Land, Antarctica.
116. Söderlund, Pia, 1999: Från gabbro till granat-amfibolit. En studie av metamorfos i Åker-metabasiten väster om Protoginzonen, Småland.

117. Jönsson, Karl-Magnus, 2000: Sedimentologiska och litostratigrafiska undersökningar i södra Malmös kvartära avlagringar, södra Sverige.
118. Romberg, Ewa, 2000: En sediment- och biostratigrafisk undersökning av den tidigare Littorina-lagunen vid Barsebäck, SV Skåne, med beskrivning av en Preboreal klimatoscillation.
119. Bergman, Jonas, 2000: Skogshistoria i Söderåsens nationalpark. En pollenanalytisk studie i Söderåsens nationalpark, Skåne.
120. Lindahl, Anna, 2000: En paleoekologisk och paleohydrologisk studie av fuktängar i Bräkneåns dalgång, Bräkne-Hoby, Blekinge.
121. Eneroth, Erik, 2000: En paleomagnetisk detaljstudie av Sarekgångsvärmen.
122. Terfelt, Fredrik, 2000: Upper Cambrian trilobite faunas and biostratigraphy at Kakeled on Kinnekulle, Västergötland, Sweden.
123. Sundberg, Sven Birger, 2000: Vattenrening genom komplexbildning mellan järn och humusämnen - en litteraturstudie med försök.
124. Sundberg, Sven Birger, 2000: Sedimentationsprocesser och avlagringsmiljö för en kantrygg kring platåleran vid Rydsgårds gods i backlandskapet söder om Romeleåsen, Skåne.
125. Kjöllerström, Anders, 2000: En geokemisk studie av bergartsvariationen på Bullberget i västra Dalarna.
126. Cinthio, Kajsa, 2000: Senglacial och tidigholocen etablering och expansion av lövträd på en lokal i nordvästra Rumänien.
127. Lamme, Sara, 2000: Klimat- och miljöförändringar under holocen i Sylarnaområdet, södra svenska Skanderna, baserat på analys av makrofossil och klyvöppningar.
128. Jönsson, Charlotte, 2000: Geologisk och hydrogeologisk modellering av området mellan Bjuv och Söderåsen, nordvästra Skåne.
129. Kleman, Johan, 2001: Utvärdering av den underkambriska litostratigrafin på Österlen, södra Sverige.
130. Sundler, Malin, 2001: En jämförande studie mellan uppmätt och MACRO-simulerad pesticidutlakning på ett odlingsfält i Skåne.
131. Grönholm, Anna, 2001: Högtrycksmetabasiter i den södra delen av Mylonitzonen: fältgeologi, petrografi och metamorf utveckling.
132. Ekdahl, Magnus, 2001: En studie av Källsjögranitens deformationsmönster och kinematiska indikatorer inom Ullaredszonen.
133. Axheimer, Niklas, 2001: Middle Cambrian trilobites and biostratigraphy of the Almbacken drill core, Scania, Sweden.
134. Lindén, Mattias, 2001: Proglacial deformation of glaciofluvial sediments during the Pomeranian deglaciation in the Neubrandenburg area, NE Germany.
135. Warnhag, Jon, 2001: A geochemical study of the zoned Pan-African Mon Repos intrusion, Central Namibia.
136. Lundmark, Mattias, 2001: Zirkonstudie av Norra Hortens bergarter, SV Sverige.
137. Gunnarson, Rebecka, 2001: Sedimentologisk undersökning av en moränskärning i en djupvittrad sprickdal på Romeleåsen, Skåne.
138. Karlsson, Christine, 2001: Diagenetic and petrophysical properties of deeply versus moderately buried Cambrian sandstones of the Caledonian foreland, southern Sweden.
139. Eriksson, Mårten, 2001: Bedömning av föroreningsspridning kring en nedlagd bensinstation i Karlaby, sydöstra Skåne.
140. Ljung, Karl, 2001: A paleoecological study of the Pleistocene-Holocene transition in the Kap Farvel area, South Greenland.
141. Åkesson, Cecilia, 2001: Undersökning av grundvattenförhållanden i området kring Östra Vemmerlöv, Simrishamns kommun, sydöstra Skåne.
142. Bermin, Jonas, 2001: Modelling Mössbauer spectra of biotite.
143. Mansurbeg, Howri, 2001: Modelling of reservoir quality in quartz-rich sandstones of the Lower Cretaceous Bentheim sandstones, Lower Saxony Basin, NW Germany.
144. Hermansson, Tobias, 2001: Sierggavággeskollans strukturgeologiska utveckling; nyckeln till Sareks berggrundsgeologi.
145. Veres, Daniel-Stefan, 2001: A comparative study between loss on ignition and total carbon analysis on Late Glacial sediments from Atteköps mosse, southwestern Sweden, and their tentative correlation with the GRIP event stratigraphy.
146. Ahlberg, Tomas, 2001: Hydrogeologisk undersökning samt sårbarhetskartering av området kring tre bergborrade grundvattenanläggningar i Simrishamns kommun.
147. Boman, Daniel, 2001: Tektonostratigrafi och deformationsrelaterad metamorfos i norra Kebnekaisefjällen, Skandinaviska Kaledoniderna.
148. Olsson, Stefan, 2002: The geology of the Portobello Peninsula; proposal of a saturated to oversaturated lineage within the Dunedin Volcano, New Zealand.
149. Molnos, Imre, 2002: Petrografi och diagenes i den underkambriska lagerföljden i Skrylle, Skåne.
150. Malmborg, Pär, 2002: Correlation between diagenesis and sedimentary facies of the Bentheim Sandstone, the Schoonebeek field, The Netherlands.